공학박사 학위논문

Treatment of hindlimb ischemia and cutaneous wound by induction of angiogenesis

혈관신생 유도를 통한 하지허혈 및 창상의 치료

2016년 8월

서울대학교 대학원

협동과정 바이오엔지니어링 전공

장 현 기

Abstract

Treatment of hindlimb ischemia and cutaneous wound by induction of angiogenesis

Hyeon-Ki Jang

Interdisciplinary Program for Bioengineering

The Graduate School

Seoul National University

Blood vessels are highly organized system that delivers oxygen and nutrients to all part of a body. A disorder of blood vessel system causes ischemic diseases including peripheral artery disease, ischemic heart disease, and stroke etc. In treating the ischemic diseases, induction of angiogenesis is promising strategy to provide blood flow in ischemic tissue and attenuate ischemic damage. Also, angiogenesis has an essential role in wound healing process. It restores vascular network system in the wound and provides nutrients and oxygen to the cells that participate in the healing process. Impaired

angiogenesis can delay healing process and result in chronic wound formation. Herein, we introduced novel methods to induce angiogenesis, which are purposed to treat mouse hindlimb ischemia and cutaneous wound.

In chapter III, conditioned medium (CM) collected from human fibrosarcoma HT1080 cell culture was used to treat mouse hindlimb ischemia. CM obtained from HT1080 cell line culture was compared with CM obtained from a human bone marrow-derived mesenchymal stem cell (MSC) culture. HT1080 CM contained higher concentrations of angiogenic factors compared with MSC CM, which was attributable to the higher cell density that resulted from a much faster growth rate of HT1080 cells compared with MSCs. For use in *in vitro* and *in vivo* angiogenesis studies, HT1080 CM was diluted such that HT1080 CM and MSC CM would have the same cell number basis. The two types of CMs induced the same extent of human umbilical vein endothelial cell (HUVEC) proliferation *in vitro.* The injection of HT1080 CM into mouse ischemic limbs significantly improved capillary density and blood perfusion compared with the injection of fresh medium. Although the therapeutic outcome of HT1080 CM was similar to that of MSC CM, the preparation of CM by tumor cell line culture would be much more efficient due to the faster growth and unlimited life-time of the tumor cell line. These data suggest the potential application of tumor cell CM as a therapeutic modality for angiogenesis and ischemic diseases.

In chapter IV, we introduced a wearable organic photovoltaic patch that can be applied on skin wound sites to promote the wound healing. Electrical stimulation by electric field (EF) can modulate behaviors of skin or immune cells. Attached to the scratched back skin of a mouse, our patch provides a constant EF maintained by photovoltaic energy harvesting from organic solar cell under the visible light illumination. *In vivo* data demonstrated the patch promoted angiogenesis in wound bed and cutaneous wound healing *via* enhanced host-inductive cell proliferation, cytokine secretion, and protein synthesis. This approach leads to a more clinically relevant, patient-friendly wearable dermal patch therapy for wound healing.

This study demonstrated that tumor cell CM injection and electric stimulation via organic photovoltaic patch could be effective method to induce angiogenesis and expect therapeutic outcome when applied to disease models. Moreover, these methods are clinically relevant since the methods are cell injection-free treatment.

Keywords: angiogenesis, ischemic disease, conditioned medium, cutaneous wound, organic photovoltaic cell

Student Number: **2010-23356**

Table of contents

List of figures

List of tables

Chapter 1.

Research backgrounds

1.1. Ischemic disease and cell therapy

Ischemic diseases including peripheral arterial disease and ischemic heart disease are caused by a disorder of blood flow. The multi potency and immunoregulatory function of mesenchymal stem cells make the stem cell therapy promising strategy for ischemic disease treatment [1]. Adipose-derived stem cell (ASC), cord blood-derived mesenchymal stem cell (CB-MSC), and hematopoietic stem cell (HPC) as well as bone marrow-derived stem cell (BM-MSC) have been proved to have therapeutic outcome in ischemic disease models [2, 3].

However, poor cell engraftment is a major problem which decreases therapeutic efficacy of stem cell transplantation [4]. In stem cell delivery for ischemic heart disease, mechanical loss due to heart beat and ischemic condition interrupt retention or survival of administered stem cells [3, 5]. The MSCs injected border zone of ischemic rat heart decreased to 27.6 ~ 46.0 % within 2 days. Also, 90% of human MSCs were detectable in healthy rat myocardium after 28 days of injection into the myocardium, whereas only 18% of those injected in the infarcted myocardium were detectable [6].

Growth factors such as vascular endothelial growth factor (VEGF) or fibroblast growth factor (FGF) have been proved to enhance cell engraftment

when these factors were delivered into ischemic region together with cells [7, 8]. Also, genetic modification was used to improve survival of transplanted cells. Overexpression of Serine/threonine protein kinase (Akt), Proto-oncogene serine/threonine-protein kinase Pim-1 (Pim-1), or Heme oxygenase-1 (HO-1) in stem cells significantly increased cell survival when transplanted into ischemic tissues [9-11]. Also, the modality of cell delivery was modified from single cells delivery into cell sheet [12, 13] or cell spheroid delivery [14, 15], which have been proved to increase cell engraftment. These results would be resulted from the presence of ECM protein that eliminated by trypsin treatment of cells. Although the advances in the cell delivery method, poor cell engraftment still remain major obstacle in cell-based therapy.

1.2. Stem cell-conditioned medium

Conditioned medium (CM) is the culture medium that has already been used by cells. Since the CM was enriched by cell secretome including growth factors, it used to support the growth of cells or induce differentiation of stem cells. Also, conditioned medium collected from stem cells could be used to treat ischemic diseases. Conditioned medium collected from stem cells contains various angiogenic factors such as VEGF, FGF, hepatocyte growth factor (HGF) or stromal cell-derived factor (SDF) [16, 17]. Moreover, the therapeutic outcome of stem cell transplantation in ischemic disease model has been proved to be responsible for the paracrine factors of stem cells [18, 19]. Thus, the use of stem cell conditioned medium was alternative strategy to bypass problems caused by poor cell engraftment. Accumulating data proved that the efficacy of stem cell conditioned medium in ischemic disease model [20]. Growth factors such as VEGF or FGF that MSCs secrete have been reported to induce angiogenesis and attenuate damages in ischemic tissues [14, 21, 22]. Also, cytokines such as interleukin 6 (IL-6), interleukin 8 (IL-8) had critical role in the treatment of hindlimb ischemia [22, 23].

1.3. Wound healing and angiogenesis

Acute wound healing process divided into 4 overlapping phases known as hemostasis, inflammation, proliferation and remodeling phases [24]. The first stage of acute wound healing is hemostasis. In this phase, bleeding is finished and a provisional wound matrix is formed. Furthermore, this phase initiates the inflammatory process. In the inflammatory phase neutrophil and monocyte are recruited into wound site and macrophage appeared. Factors secreted by the neutrophil or monocyte/macrophage triggers proliferation of cellular and structural components. The main processes of the proliferation phase are the recovering of the wound surface, the formation of granulation tissue and the restoration of the vascular network. Finally in the remodeling phase, extracellular matrix protein is remodeled to provide strength to the wound and decrease wound thickness [25]. The underlying connective tissue shrinks in size and the wound margins become closer together.

During the proliferative phase, wound microvasculature is reconstructed by angiogenesis in order to re-establish the nutrient supply to regenerating tissue, where fibroblast proliferation and ECM synthesis occur. Impaired angiogenesis will result in delayed wound healing. [26, 27]

1.4. Wound electric field

All cells generate a voltage across their plasma membranes called the membrane potential. Skin cells also generate a voltage, but the multi-layered constructs of skin cells generate a voltage across skin epithelium. This voltage, termed the transepithelial potential (TEP) are attributed to the polarized distribution of ion channels in the epithelial cells. Most Na^+ channels are localized to the apical membrane and most K^+ channels are found in the basolateral membranes along with the Na^+/K^+-ATPase (Figure 1.1.). The Na^+/K^+-ATPase operates to maintain high internal K^+ and low internal Na^+. Thus the localization of channels results in K^+ efflux across the basolateral membrane and Na^+ influx across the apical membrane. This ion flux constitutes transepidermal ion flux and creates a TEP of between 20 ~ 50 mV [28]. When the skin epithelium was wounded, leakage current will occur caused by the TEP through low resistance pathway created by the wound (Figure 1.2.). This positive wound current flows toward the wound on the basal side of the epidermis, and then away from the wound on the apical side, while a lateral electric field is generated by this flow of wound current. The range of electric field strength is between 40 ~ 200 mV/mm [29].

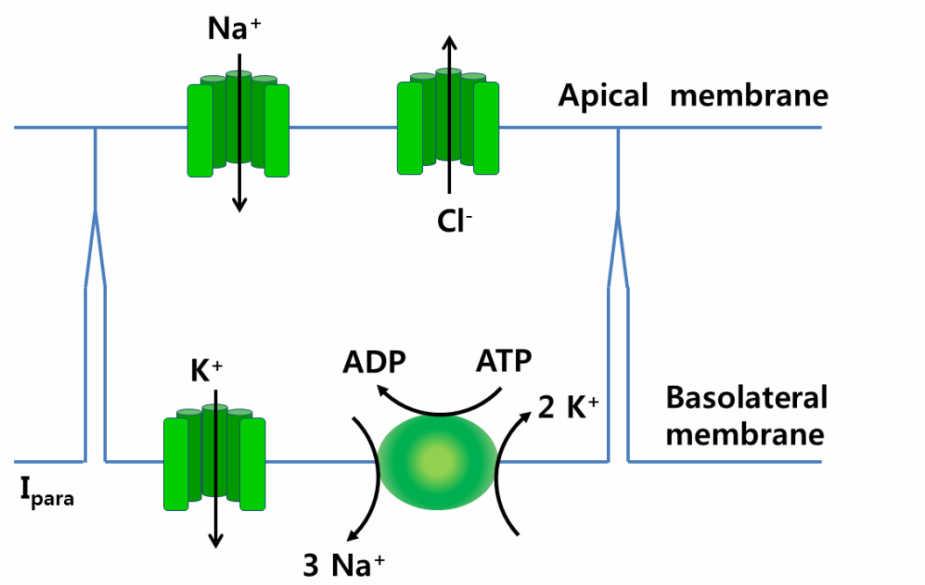

Figure 1.1. Typical epithelial cell in a monolayer with Na^+ and Cl^- channels localized on the apical plasma membrane and K^+ channels localized on the basolateral membranes along with the Na^+/K^+-ATPase.

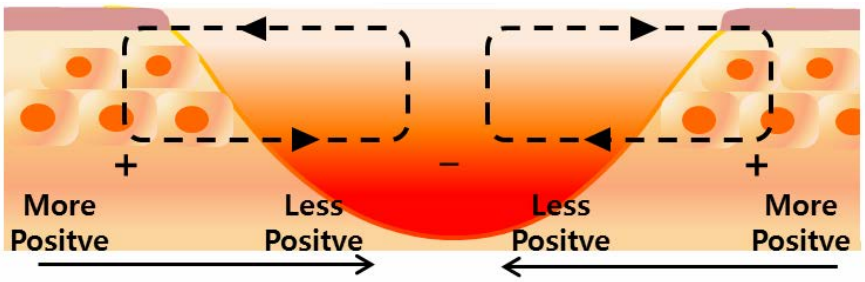

Figure 1.2. Generation of wound electric field

1.5. Electrical stimulation for wound treatment

Since the existence of wound currents was demonstrated in 1843 [30], application of electrical stimulation on wound healing has been researched. As the number of reports about in vivo wound healing model, clinical trials increased and the concept of using electrical stimulation for the treatment of wound has become widely accepted. In 2002 in the United States, ES was approved for payment by the Centers for Medicare and Medicaid Services for the treatment of pressure ulcers and wounds of the lower extremity caused by venous and arterial insufficiency and diabetes that have not responded to standard wound treatment.

Two types of electrical stimulation on wound healing are usually defined: continuous direct current (CDC) and pulsed current (PC) [31]. CDC studies that are applied between 200 and 800 μA have been reported to have positive wound-healing outcomes in a number of clinical trials [30, 32, 33]. Pursed current has various types of waveform depending on its frequency, amplitude, or duration time. In the cases of high-voltage pulsed current, voltage about 100 ~ 360 V and duration time within 100 μs have been reported to improve wound healing [34].

Most of these studies utilized large-sized devices to deliver electric stimulation on the injury site and required hospitalization of the patients. In contrast, most commercialized dermal patches are wearable size but only focus on minimizing tissue infections and rehydrating the wound sites [35]. Therefore, the development of a wearable device that can deliver electric stimulation at the wound site can allow patient-friendly clinical application of electric stimulation therapy for wound healing.

Chapter 2.

Experimental Procedure

2.1. Cell Preparation

2.1.1. HT1080 human fibrosarcoma cell culture

HT1080 human fibrosarcoma cells (American Type Culture Collection (ATCC), Manassas, VA, USA) were cultured in Dulbecco's modified Eagles medium (DMEM, Gibco BRL, Gaithersburg, MD, USA) supplemented with 10 % (v/v) fetal bovine serum (FBS, Gibco BRL), 100 units/ml of penicillin (Gibco BRL), and 100 μg/ml of streptomycin (Gibco BRL). To evaluate a growth rate of HT1080 cells, the cells were plated on culture dishes at a density of 5×10^3 cells/cm^2. The cell numbers were determined using a hemocytometer at days 1, 3, 5, and 7 in triplicate samples (n = 3). The cell doubling times were calculated using the formula: $t \cdot (\ln 2)/(\ln N_2 - \ln N_1)$, where t is time period of culture and N_1 and N_2 are cell numbers at the first and second time points, respectively.

2.1.2. Human mesenchymal stem cell (MSC) culture

Bone marrow-derived human MSCs (hMSCs, Lonza, Walkersvile, MD, USA) were cultured in DMEM (Gibco BRL, Gaithersburg, MD, USA) supplemented with 10 % (v/v) FBS (Gibco BRL), 100 units/ml of penicillin (Gibco BRL), and 100 μg/ml of streptomycin (Gibco BRL). All experiments were performed using MSCs within seven passages. To evaluate a growth rate of MSCs (passage number = 7), the cells were plated on culture dishes at a density of 5×10^3 cells/cm^2. The cell numbers were determined using a hemocytometer at days 1, 3, 5, and 7 in triplicate samples (n = 3). The cell doubling times were calculated using the formula: $t \cdot (\ln 2)/(\ln N_2 - \ln N_1)$, where t is time period of culture and N_1 and N_2 are cell numbers at the first and second time points, respectively.

2.1.3. Human umbilical vein endothelial cells (HUVECs) culture

HUVECs (Lonza, Allendale, NJ, USA) were cultured in endothelial growth medium (EGM-2, Lonza) supplemented with 100 units/ml of penicillin (Gibco BRL), and 100 μg/ml of streptomycin (Gibco BRL).

2.1.4. Human dermal fibroblasts (HDF) culture

HDF (Lonza) were cultured in DMEM (Gibco BRL, Gaithersburg, MD, USA) supplemented with 10 % (v/v) FBS (Gibco BRL), 100 units/ml of penicillin (Gibco BRL), and 100 μg/ml of streptomycin (Gibco BRL). All experiments were performed using HDFs within seven passages.

2.2. Conditioned medium (CM) preparation

CMs were prepared by MSC culture and HT1080 cell culture following the procedures described in previous studies [36, 37]. Cells were plated on culture dishes at an over-confluent density (4×10^4 cells/cm^2) in the 10 % FBS-containing medium and allowed for cell adhesion for two days. Then, the medium was removed, and the cells were washed with serum-free DMEM (Gibco BRL) twice to remove serum components. After the medium was replaced with serum-free DMEM (Gibco BRL), the cells were incubated under hypoxic conditions (3 % O_2) to stimulate angiogenic factor secretion, [36, 37] and the CM was collected after 24 hr. To remove cells from CM, the collected CM was centrifuged at 500 × g for 10 min and filtered through a 0.22 μm filter (Corning Inc., Corning, NY, USA).

For *in vitro* and *in vivo* angiogenesis studies, HT1080 CM was diluted with DMEM so that HT1080 CM and MSC CM had the same cell numbers at a concentration of 1 ml medium per 3.3×10^6 cells. All CMs used in the experiment were freshly prepared, stored at 4°C, and used within 1 week.

2.3. Wearable organic photovoltaic patch fabrication

2.3.1. Organic solar cell fabrication

The fabrication method of organic solar cells was followed by previously reported our procedure [38]. Zinc oxide (ZnO) as electron transport layer was deposited by sol-gel method on patterned ITO-glass substrate. Photoactive solution (P3HT:PCBM, 2 wt%, 1:1 w/w, in m-xylene) was spin-coated on ZnO/ITO glass substrate. PEDOT:PSS layer (40 nm) was then spin-coated on the photoave layer (150 nm) as hole transport layer and the substrate thermally annealed at 150 °C for 10 min. in a N_2 atmosphere. Ag electrode was thermally evaporated on PEDOT:PSS layer as a top electrode under high vacuum (low 10^{-6} torr). Three individual photovoltaic devices with 16 mm^2 area/ea were connected in parallel in a substrate. The organic solar cells were finally encapsulated by epoxy for ambient stability with metal wire to connect with wound healing electrodes.

2.3.2. Wound healing electrode preparation and patch integration

Two concentric circle electrodes plated with Au were molded on the surface of PDMS elastomer substrate with metal wire to connect with cathode and anode of organic solar cell. Inner one is located in the center of PDMS substrate diameter and had 4 mm of diameter. The outer one had 15 mm inner circle diameter and 3 mm of thickness. The organic solar cell and wound healing electrode were connected by metal wire welding. The two parts were integrated by filling the gap of two parts with PDMS elastomer.

2.3.3. Characterization

The photovoltaic characteristics of the patch were measured using Keithley 2400 source measurement device under white LED light (DI-LED-6W, SFS Lights, China) in air.

2.4. In vitro assays

2.4.1. Viability of cells at varied initial cell density

For the comparison of cell viability at varied initial cell seeding density, MSCs and HT1080 cells were plated on culture dishes at 1×10^4 cells/cm^2 and 4×10^4 cells/cm^2. Then, the cells underwent the same procedure of the preparation of CM as described above. In brief, the cells were cultured in the 10 % FBS-containing medium under normoxic condition for two days and incubated in the serum-free medium under hypoxic conditions (3 % O_2) for 24 hr for the preparation of the CMs. The cells were trypsinized before (day 2) and after (day 3) the hypoxic incubation, and stained with trypan blue dye (Sigma Aldrich) for cell viability evaluation. Then, the cell numbers were determined using a hemocytometer in triplicate samples.

For western blot analysis, the CMs were concentrated by centrifugation using centrifugal filters (Amicon Ultra, Millipore Corp., Bedford, MA) and total volume was normalized upon the cell numbers at day 2. MSC lysate was prepared using sodium dodecyl-sulfate (DS) sample buffer (62.5 mM Tris-HCl (pH 6.8), 2% (w/v) SDS, 10% (v/v) glycerol, 50 mM dithiothreitol, and 0.1% (w/v) bromophenol blue). The total concentration of the protein was determined with bicinchoninic acid protein assay (Pierce Biotechnology, Rockford, IL) and further performed through 10% (w/v) SDS-polyacrylamide

gel electrophoresis. Proteins were transferred to Immobilon-P membrane (Millipore Corp.) and probed with antibodies against beta-actin (ß-actin; Abcam, Cambridge, U.K.). Proteins were incubated with horseradish peroxidase-conjugated secondary antibody (Santa Cruz Biotechnology, Santa Cruz, CA) for 1 h at room temperature, and blots were developed using a chemiluminescence detection system (Amersham Bioscience, Piscataway, NJ).

2.4.2. Profile of cytokines and angiogenic factors in CMs

Cytokines and angiogenic factors in the MSC CM and HT1080 CM were characterized using the Proteome Profiler™ Human Cytokine Array Panel A (R&D Systems Inc., Minneapolis, MN, USA) and Profiler™ Human Angiogenesis Array (R&D Systems Inc.) according to the manufacturer's instructions. Chemiluminescent signals were detected by using Gel Logic 2200 PRO (Carestream, Rochester, NY, USA). Analysis for each antibody array was performed in triplicate using independent samples and quantified with densitometry.

2.4.3. HUVEC culture with CMs

Human umbilical vein endothelial cells (HUVEC, Lonza, Allendale, NJ, USA) were plated at a density of 5×10^3 cells/cm^2 on 4-well chamber slides containing endothelial growth medium (EGM-2, Lonza) that contained 2 % (v/v) serum and allowed for cell adhesion for 24 hr. After HUVECs were serum-starved for 8 hr in endothelial growth basal medium (EBM-2, Lonza), each well received 10 μl of HT1080 CM or MSC CM, which was produced by 3.3×10^4 HT1080 cells or MSCs. In the negative control group, 10 μl of phosphate buffered saline (PBS, Sigma Aldrich) was added to each well. In the positive control group, EBM-2 (Lonza) was replaced with EGM-2 (Lonza). For growth factor neutralization experiments, HUVECs were cultured with EBM-2 plus HT1080 CM supplement containing antibodies (5 μg/ml, R&D Systems Inc.) against VEGF, placental growth factor (PLGF), or granulocyte macrophage colony-stimulating factor (GM-CSF) or IgG. Then, all of the groups were incubated for 24 hr, and the HUVECs were washed with PBS (Sigma Aldrich) and fixed in 4 % (w/v) para-formaldehyde (PFA) for 10 min for characterization.

2.4.4. Immunocytochemistry

For the quantification of proliferating cells, HUVECs were fixed with 4 % (w/v) PFA and subjected to immunofluorescent staining with anti-PCNA antibodies (Abcam, Cambridge, UK). Fluorescein isothiocyanate–conjugated secondary antibodies (Jackson ImmunoResearch, West Grove, PA, USA) were used to visualize the signals. The cells were counterstained with 4',6-diamidino-2-phenylindole (DAPI, Vector Laboratories, Burlingame, CA, USA) and examined using a fluorescence microscope (IX71, Olympus, Tokyo, Japan).

2.4.5. Electrical stimulation on dermal fibroblast

Electric chamber was manufactured following previous method [39]. Fibroblasts were seeded in the chambers and incubated up to 24 hours, allowing them to settle and adhere to the chamber. Scratches were made on each monolayer of fibroblasts and the culture medium was refreshed. Then the linear power supplier (GPC-1850D, Good Will Instrument, New Taipei City 236, Taiwan) was used to apply current through the chamber. The cultures were photographed at 0 and 6 hr after electrical stimulation. The applied current was 0.01 A/cm^2, corresponding to 70 mV/mm field strength [39]. Then the cells were further cultured for 18h without electric stimulation for the analysis of gene expression.

2.4.6. Quantitative real-time polymerase chain reaction (qRT-PCR)

qRT-PCR was used to quantify the relative gene expression levels of *PCNA* and *Fibronectin* (n = 5). Total ribonucleic acid (RNA) was extracted from samples using 1 mL Trizol reagent and 200 μL chloroform. The lysed samples were centrifuged at 12,000 rpm for 10 min at 4 °C. The RNA pellet was washed with 75 % (v/v) ethanol in water and dried. After drying, samples were dissolved in RNase-free water. For qRT-PCR, the iQ™ SYBR Green Supermix kit (Bio-Rad, Hercules, CA, USA) and the MyiQ™ single color real-time PCR detection system (Bio-Rad) were used. *β-actin* served as the internal control.

2.5. Experimental procedures *in vivo*

2.5.1. Mouse hindlimb ischemia model

Six-week-old female athymic mice (20–25 g body weight, Orient, Seoul, Korea) were anesthetized with xylazine (10 mg/kg) and ketamine (100 mg/kg). The femoral artery and its branches were ligated using a 6-0 silk suture (Ethicon, Somerville, NJ, USA). The external iliac artery and all of the upstream arteries were then ligated. The femoral artery was excised from its proximal origin as a branch of the external iliac artery to the distal point from where it bifurcates into the saphenous and popliteal arteries. All animal treatments and experimental procedures were approved by the Institutional Animal Care and Use Committee of Seoul National University (No. SNU-130219-7).

2.5.2. Treatment of limb ischemia

The ischemic hindlimbs of the mice were treated with a method modified from a procedure described in a previous study [40]. Immediately after arterial dissection, the mice were randomly divided into four groups (n = 5 animals per group): Fresh medium (FM), MSC, MSC CM or Tumor CM. The MSC group received a single injection of human MSC suspension (100 μl, 1×10^6 cells in DMEM) into the gracilis muscle in the medial thigh at day 0. The FM group, MSC CM group and Tumor CM group received a daily injection of 100 μl of FM (DMEM), MSC CM, and HT1080 CM, respectively, for 6 days. Each mouse in the HT1080 CM group and MSC CM group received a daily injection of CM obtained from the culture of 2×10^6 HT1080 cells and 2×10^6 MSCs, respectively, for 6 days, which was less than the cell number (1×10^6 cells) of the MSC injection group because implanted MSCs are known to secrete angiogenic factors for longer periods (c.a., 2 weeks) [18].

2.5.3. Mouse skin wound model

Six-week-old female athymic mice (20–25 g body weight, Orient, Seoul, Korea) were anesthetized with xylazine (20 mg/kg) and ketamine (100 mg/kg). An 12 mm round full-thickness excisional wound was made on the dorsal back of each mouse. Epidermis, dermis, subcutaneous tissue, and panniculus carnosus were removed, and the muscle tissue was exposed. Four knots (6-0 sutures; Ethicon, Somerville, NJ) were tied at the boundary of the wound. All animals received care according to the “Guide for the Care and Use of Laboratory Animals” of Seoul National University. This animal study was performed with permission from the Institutional Animal Care and Use Committee at Seoul National University (SNU-160304-6).

2.5.4. Treatment of mouse skin wound

After the full-thickness excisional wound was made, mice were randomly assigned to one of three treatments as follows: wound dressing (WD), electrode only (E), or wearable OPP (SC). Wound lesion of WD group was dressed with transplant Tegaderm film (Tegaderm™, 3M Health Care) and the PDMS substrate was attached to the wound site. Wound lesion of SC group was dressed with the Tegaderm film (3M Health Care) and treated with the wearable OPP. The electrode directly contacted with wound lesion or normal skin of border zone to deliver electrical signal on the wound. Wound lesion of E group was also dressed with the Tegaderm film (3M Health Care) and treated with the electrode part that has no solar cells to generate electrical stimulation. The electrode directly contacted with wound lesion or normal skin of border zone. After the treatments, all groups were dressed again with the Tegaderm film (3M Health Care) to attach the device on the wound site. The lamps were controlled to switch on/off at 12 hours period according to the “Guide for the Care and Use of Laboratory Animals” of Seoul National University. Wound healing statuses were followed up to 12 days after the treatment. At minimum every three days, the Tegaderm film (3M Health Care) was replaced new one and electrode part was cleaned by using ethanol-soaked gauze. Wound lesion was wet by sterile PBS-soaked gauze to prevent drying

while the Tegaderm film (3M Health Care) was replaced. All samples were collected in identical manner to compare the wound healing differences among the groups. Entire tissues in the dorsal wound area were retrieved for analyses to compare the wound healing processes occurred in the wound area among the groups.

2.6. Laser Doppler imaging analysis

Laser Doppler imaging analysis was performed with a laser Doppler perfusion imager (Moor Instruments, Devon, UK) for serial noninvasive physiological evaluation of neovascularization. The mice were monitored by serial scanning of surface blood flow in the hindlimbs on days 0, 3, 7, 14, and 28 after treatment. The digital color-coded images were analyzed to quantify blood flow in the region from the knee joint to the toe, and the mean values of perfusion were subsequently calculated (n = 5 animals per group).

2.7. Histological examination

2.7.1. Immunohistochemistry for hindlimb

The thigh muscles in the ischemic limbs of the mice were harvested at 28 days after treatments. The samples were fixed in 4 % (w/v) PFA followed by incubation in a series of 15 % (w/v) and 30 % (w/v) sucrose solution in PBS (Sigma Aldrich). Then, the samples were embedded in optimal cutting temperature compound (OCT compound, Tissue-Tek 4583, Sakura Finetek USA Inc., Torrance, CA, USA), frozen at -80 °C, and sliced to a thickness of 10 μm at -22 °C. For the quantification of microvessels in the ischemic regions, the sections were subjected to immunofluorescent staining with anti-CD31 antibodies (Abcam). Fluorescein isothiocyanate–conjugated secondary antibodies (Jackson ImmunoResearch) were used to visualize the signals. The specimens were counterstained with DAPI (Vector Laboratories) and examined using a fluorescence microscope (Olympus).

2.7.2. Histological examination for skin wound

The tissues of the wound regions were retrieved 12 days after the treatments. The tissues were fixed in 10 % (v/v) buffered formaldehyde, dehydrated using a series of graded ethanol, embedded in paraffin, and sliced into 4-μm thick sections. Microscopic tissue-regeneration was evaluated using Masson trichrome- or H&E-stained tissue sections and a light microscope (KS400, Zeiss). The intersubcutaneous distance was measured (n = 4 different samples per group) on digital images using the imaging software software ImageJ (NIH, Bethesda, MD, USA).

2.7.3. Immunohistochemistry for skin wound

The tissues of the wound site were retrieved 12 days after the treatment and embedded in an optimal cutting temperature compound (TISSUE-TEK® 4583, Sakura Finetek USA Inc., Torrance, CA, USA), followed by freezing and slicing into 10 μm thick sections at -22 °C. Immunohistochemistry was performed against laminin (Abcam, Cambridge, UK) and involucrin (Abcam) to examine the regeneration of the basal layer and epidermis, respectively. The staining signals for laminin and involucrin were visualized using fluorescein-isothiocyanate-conjugated or rhodamine-conjugated secondary antibodies (Jackson Immuno Research Laboratories, West Grove, PA, USA), respectively. To assess the microvessel density, tissue sections were stained with antibodies against Von Willebrand factor (vWF, Abcam). vWF-positive signals were visualized using fluorescein-isothiocyanate-conjugated secondary antibodies (Jackson Immuno Research Laboratories). Tissue sections were mounted in DAPI (Vector Laboratories). A fluorescent microscope (Olympus) was used to count the microvessels. Four different images per slide from 20 random slides were randomly analyzed for each group (n = 4 different samples per group) for immunohistochemical quantification.

2.8. Morphometric analysis

The macroscopic wound area was quantified by processing photographs obtained at various time points (day 0, 3, 6, 9, and 12) by tracing the wound margin and calculating the pixel area. The location of the advancing margin of wound closure was defined as the grossly visible margin of epithelial migration toward the center of the wound and over the granulation tissue bed. The wound area was calculated (n = 8 different samples per group) as the percentage of the initial wound area ([wound area at time] / [initial wound area] × 100 %). Morphometric analysis was performed based on the digital images using the imaging software ImageJ (NIH).

2.9. Western blot analysis

Tissue samples were obtained from the mouse wound area 12 days after the treatments, and homogenized using a Dounce homogenizer (50 strokes, 4 °C) in ice-cold lysis buffer (15 mM Tris-HCl, pH 8.0, 0.25 M sucrose, 15 mM NaCl, 1.5 mM $MgCl_2$, 2.5 mM ethylenediaminetetraacetic acid, 1 mM ethylene glycol tetraacetic acid, 1 mM dithiothreitol, 2 mM NaPPi, 1 mg/mL of pepstatin A, 2.5 mg/mL of aprotinin, 5 mg/mL of leupeptin, 0.5 mM phenylmethyl sulfonyl fluoride, 0.125 mM Na_3VO_4, 25 mM NaF, and 10 mM lactacystin). The protein concentration was determined using a bicinchoninic acid protein assay (Pierce Biotechnology, Rockford, IL, USA). Western blot analysis was performed using 10 % sodium dodecyl sulfate-polyacrylamide gel electrophoresis. After the proteins were transferred onto an Immobilon-P membrane (Millipore Corp., Billerica, MA, USA), they were probed with antibodies against laminin, involucrin, caspase-3, CD68, mouse VEGF, PCNA, COL III, TGF-β, CD99, Iα5, matrix metalloproteinase-2 (*MMP-2*), fibronectin, COL IV, COL I, and β-actin (all antibodies were purchased from Abcam) and incubated with a horseradish peroxidase-conjugated secondary antibody (Santa Cruz Biotechnology, CA, USA) for 1 hr at room temperature. The blots were developed using an enhanced chemiluminescence detection system (Amersham Bioscience, Piscataway, NJ, USA). Luminescence was recorded

on X-ray film (Fuji super RX, Fujifilm Medical Systems, Tokyo, Japan) and the bands were imaged and quantified (n = 5 different samples per group) using an Imaging Densitometer (Bio-Rad).

2.10. Statistical analysis

The quantitative data were expressed as mean ± standard deviation. The statistical significance was evaluated with the Mann Whitney test for comparison of cytokines and angiogenic factor content between MSC CM and HT1080 CM. Statistical analysis among multiple groups was performed using ANOVA followed by a Bonferroni test. A probability value of $p < 0.05$ was considered significant

Chapter 3.

Induction of angiogenesis using tumor cell-conditioned medium

3.1. Introduction

Stem cell-based therapy represents a promising strategy for treating ischemic diseases due to the angiogenic properties of stem cells. Stem cells such as bone marrow-derived mesenchymal stem cells (MSCs), adipose-derived stem cells (ASCs), or endothelial progenitor cells (EPCs) implanted in the ischemic region successfully induce neovascularization and attenuate ischemic damage [18, 41-43]. However, poor engraftment of the implanted stem cells remains one of the major challenges in stem cell-based therapy [44, 45]. An option to bypass this obstacle is the injection of stem cell-conditioned medium (CM). Accumulating data suggest that significant improvements in ischemic diseases after stem cell injection are mainly attributable to the angiogenic factors secreted by the implanted cells [18, 21]. Indeed, the injection of CM collected from the cultures of stem cells, such as MSCs, ASCs, EPCs, and dental pulp stem cells, induces therapeutic angiogenesis [17, 22, 46-49].

Tumor cells can be an alternative cell source to produce therapeutic CM for angiogenesis and ischemic disease treatment. Growing tumors secrete pro-angiogenic factors, such as vascular endothelial growth factor (VEGF) and fibroblast growth factors (FGF), to recruit blood vessels for oxygen and nutrient supply [50, 51]. Accordingly, the angiogenic activity of tumor cell CM has been demonstrated in a number of studies. CM collected from the

cultures of pulmonary carcinoma cells and fibrosarcoma cells enhanced the proliferation and tube formation of vascular endothelial cells *in vitro* [36, 52]. Herein, we evaluated the potential of tumor cell CM for therapeutic angiogenesis and ischemic disease treatment. CM was prepared from a human fibrosarcoma HT1080 cell culture. The paracrine factor profile of HT1080 cell CM was compared with that of MSC CM, which has previously been reported to induce therapeutic angiogenesis [53]. The therapeutic efficacy of HT1080 CM was evaluated in a mouse hindlimb ischemia model and compared with that of MSC CM and MSC implantation.

3.2. Results

3.2.1. Growth of MSCs and HT1080 cells

MSCs and HT1080 cells were seeded on tissue culture plates and cultured for 7 days. The growth curves approached plateaus at day 7 (Figure 1A). The doubling times of MSCs and HT1080 cells between day 1 and 3 of culture were 47.6 hr and 8.6 hr, respectively. HT1080 cells formed multiple cell-layers, while MSCs formed a monolayer at day 7 (Figure 1B).

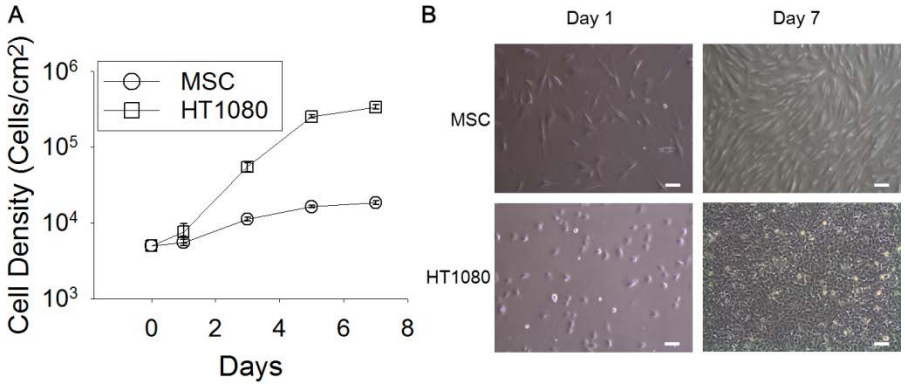

Figure 3.1. The comparison of the cell growth rate between MSCs and HT1080 cells. (A) The growth curves of MSCs and HT1080 cells during 7 days of culture. (B) The morphology of MSCs and HT1080 cells on days 1 and 7 after seeding at a density of 5×10^3 cells/cm^2 (Bars = 100 μm).

3.2.2. Viability of cells at varied initial cell seeding density

To examine the possible CM contamination with intracellular proteins that can be induced by cell death and subsequent intracellular protein exposure, we evaluated the cell viability and CM contamination using the trypan blue exclusion assay and western blot assay. As shown in figure 3.2.A, both MSCs and HT1080 showed no morphological cell death under low or high density cell seeding at day 2 and even at day 3. To further evaluate the cell viability quantitatively, we performed trypan blue exclusion assay at day 2 and 3 (Figure 3.2.B). At day 2, a slight decrease in cell viability was observed between MSCs and HT1080 under high density cell seeding. On day 3 when CM was collected, however, MSCs and HT1080 grown at high density cell seeding showed increased cell survival compared to HT1080 grown at low density cell seeding. We speculated this is because cell culture condition change on day 2, from normoxia serum-containing medium to hypoxia serum-free medium, may have caused cell death in low density cell seeding. Next, to evaluate whether cell death observed in day 2 and 3 induced CM contamination, we performed western blotting on CM collected on day 3 for all groups (Figure 3.2.C). Compared to the normal cell lysate control group, CM collected from high or low density cell seeding at day 3 showed no protein expression of beta actin, which is secreted upon cell death. This data

shows that even though partial cell viability decrease was observed in a number of groups on day 2 and 3, final product of CM for all groups showed no severe contamination with intracellular protein.

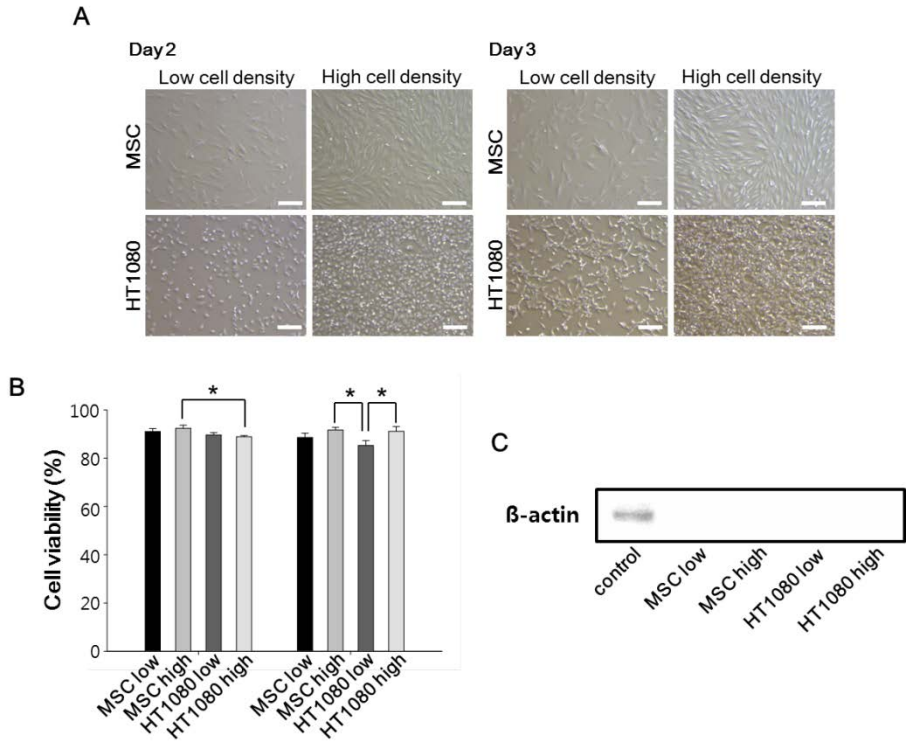

Figure 3.2. The viability of MSCs and HT1080 cells after seeding at different density. (A) Representative images of microscopic observation of cells plated at a low (1×10^4 cells/cm^2) or high (4×10^4 cells/cm^2) initial cell density at day 2 and 3. Bars = 200 μm. (B) Cell viability evaluated by trypan blue exclusion assay (*$p < 0.05$). (C) A representative image of beta-actin in the CMs analyzed by western blot. The control group was lysate of MSCs.

3.2.3. Cytokines in CMs collected from cultures of HT1080 cells and MSCs

To characterize the cytokines in the media collected from the cultures of HT1080 cells and MSCs, the CMs were analyzed using an antibody array. The relative amounts of pro-angiogenic cytokines, such as interleukin 6 (IL-6), interleukin 8 (IL-8), monocyte chemotactic protein 1 (MCP-1), and macrophage migration inhibitory factor (MIF) [22, 23, 54], were analyzed (Figure 3.3.A). The amounts of IL-6 and IL-8 per CM volume and per cell were significantly higher in MSC CM than in HT1080 CM. In contrast, the amount of MCP-1 per CM volume was significantly higher in HT1080 CM than in MSC CM, whereas no significant difference in the amounts of MCP-1 per cell was observed between HT1080 CM and MSC CM. The amount of MIF per cell was significantly higher in MSC CM than in HT1080 CM.

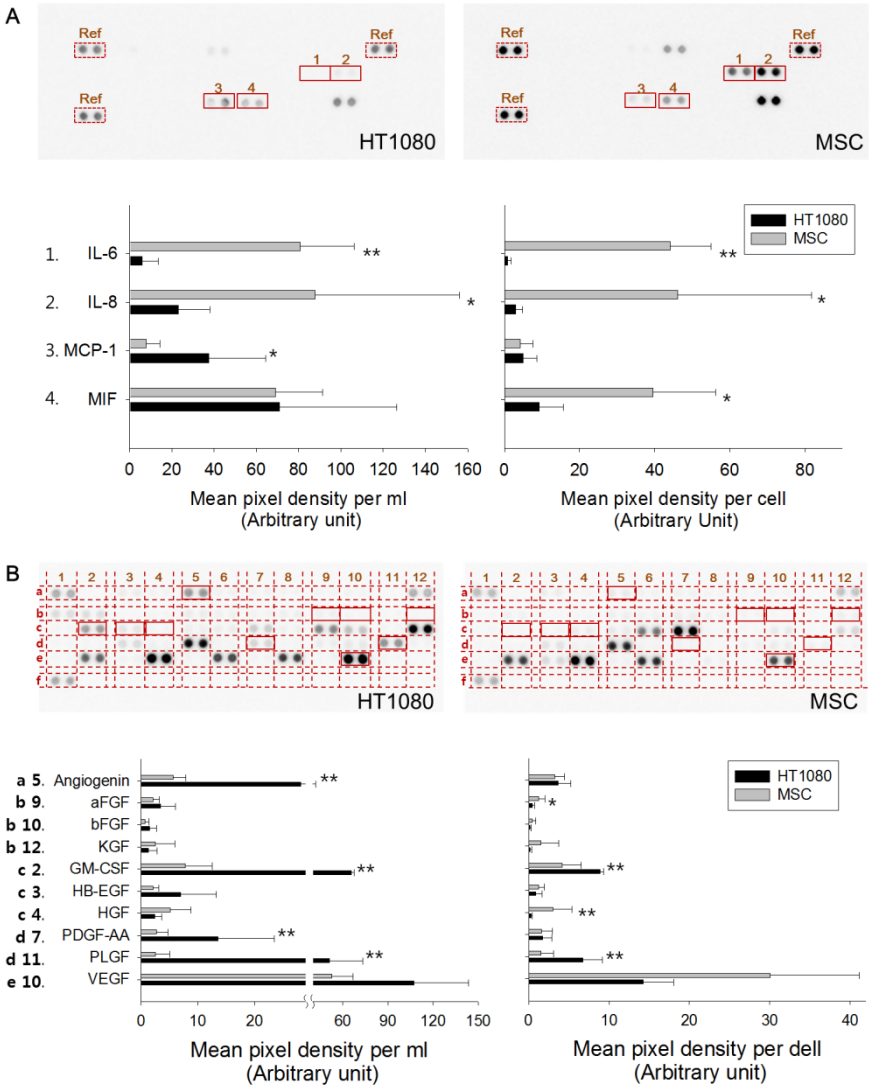
A
Ref
Ref
Ref
Ref
1
2
3
4
HT1080
MSC
HT1080
MSC
1. IL-6
2. IL-8
3. MCP-1
4. MIF
**
*
*
**
*
*
0 20 40 60 80 100 120 140 160
Mean pixel density per ml
(Arbitrary unit)
0 20 40 60 80
Mean pixel density per cell
(Arbitrary Unit)
B
1 2 3 4 5 6 7 8 9 10 11 12
a
b
c
d
e
f
HT1080
MSC
a 5. Angiogenin
b 9. aFGF
b 10. bFGF
b 12. KGF
c 2. GM-CSF
c 3. HB-EGF
c 4. HGF
d 7. PDGF-AA
d 11. PLGF
e 10. VEGF
**
**
**
**
*
**
**
**
0 10 20 60 90 120 150
Mean pixel density per ml
(Arbitrary unit)
0 10 20 30 40
Mean pixel density per dell
(Arbitrary unit)

Figure 3.3. The characterization of CMs collected from cultures of HT1080 cells and MSCs after 1 day of incubation under hypoxic conditions (3 % O_2). (A) The cytokine profiles of CMs collected from cultures of HT1080 cells and MSCs. Representative images of antibody array and quantification of the cytokine pixel density per CM volume (ml) or per cell number basis (*P < 0.05, **P < 0.01). (B) The angiogenesis-associated factor profiles of CMs collected from cultures of HT1080 cells and MSCs. Representative images of antibody array and the quantification of the factor pixel density per CM volume (ml) or per cell number basis (*P < 0.05, **P < 0.01).

3.2.4. Angiogenic factors in CMs collected from cultures of HT1080 cells and MSCs

To further characterize angiogenic factors in the CMs collected from the cultures of HT1080 cells and MSCs, the CMs were analyzed using an angiogenic factor array. The relative amounts of pro-angiogenic growth factors, such as angiogenin, acidic FGF (aFGF), basic FGF (bFGF), keratinocyte growth factor (KGF), GM-CSF, heparin-binding epidermal growth factor-like growth factor (HB-EGF), hepatocyte growth factor (HGF), platelet-derived growth factor-AA (PDGF-AA), PLGF, and VEGF[17, 55-63], were analyzed (Figure 3.3.B). The amounts of angiogenin, GM-CSF, PDGF-AA, and PLGF per CM volume were significantly higher in HT1080 CM than in MSC CM, whereas no angiogenic factor secretion was higher in MSC CM than in HT1080 CM when evaluated on a per CM volume basis. Moreover, the amounts of GM-CSF and PLGF were also significantly higher in HT1080 CM than in MSC CM when evaluated on a per cell number basis. The amounts of aFGF and HGF per cell were significantly higher in MSC CM than in HT1080 CM, though no difference was observed between MSC CM and HT1080 CM when evaluated on a per CM volume basis.

3.2.5. Enhanced proliferation of human endothelial cells in vitro by CM

In HUVEC cultures supplemented with MSC CM or HT1080 CM, the number of proliferating cells increased compared with those cultured in EBM-2 (Figure 3.4.). However, the ability of HT1080 CM and MSC CM to enhance HUVEC proliferation was lower than that of EGM-2, which is a commercial endothelial cell culture medium. No significant difference in the mitogenic activity was observed between MSC CM and HT1080 CM.

To confirm that angiogenic factors present in the CMs contributed to the enhanced proliferation of HUVECs *in vitro* in the HT1080 CM group, neutralizing antibodies were used to block VEGF, PLGF, and GM-CSF which were abundant in the HT1080 CM (Figure 3.3.B). The neutralization of VEGF and GM-CSF significantly decreased HUVEC proliferation compared with that of HT1080 CM group (Figure 3.4.). However, when PLGF was neutralized, HUVEC proliferation was not significantly changed compared with that of the HT1080 CM group.

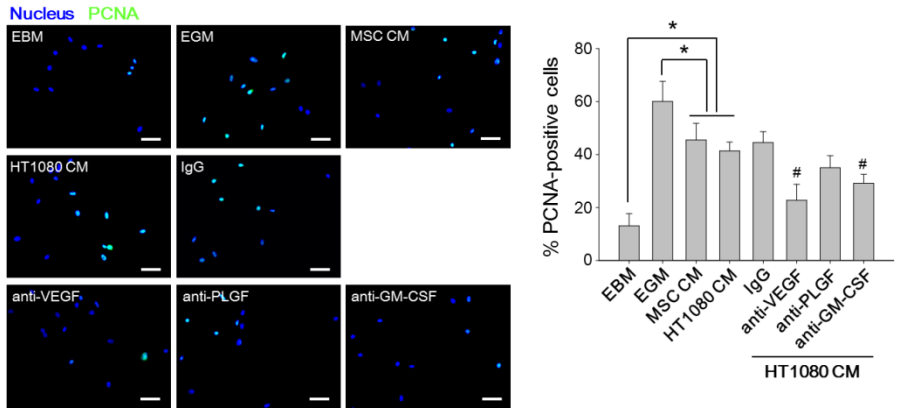

Figure 3.4. The proliferation of HUVECs cultured for 24 hr with EBM, EGM-2, MSC CM, HT1080 CM, HT1080 CM containing antibody against VEGF, HT1080 CM containing antibody against PLGF, HT1080 CM containing antibody against GM-CSF, or HT1080 CM containing IgG. HT1080 CM was diluted with DMEM such that HT1080 CM and MSC CM had the same cell number basis. The proliferating cells were stained with PCNA antibody (light green). Blue indicates nuclei stained with 4',6-diamidino-2-phenylindole (DAPI) (Bars = 50 μm. *$p < 0.05$, #$p < 0.05$ versus HT1080 CM).

3.2.6. Angiogenesis in the ischemic limbs by CM injection

To evaluate the therapeutic potential of HT1080 CM in mouse hindlimb ischemia models, mice were treated with either a single injection of MSCs or a daily injection of 100 μl of FM, MSC CM or HT1080 CM for 6 days into the gracilis muscle following the induction of hindlimb ischemia. Twenty-eight days after the treatment, the number of CD31-positive capillaries was evaluated in the ischemic region (Figure 3.5.A). The capillary density was significantly increased after treatment with HT1080 CM compared to treatment with FM. The treatments with MSCs and MSC CM also significantly enhanced the capillary density compared to treatments with FM. There was no significant difference in the capillary density among the MSCs, MSC CM and HT1080 CM groups.

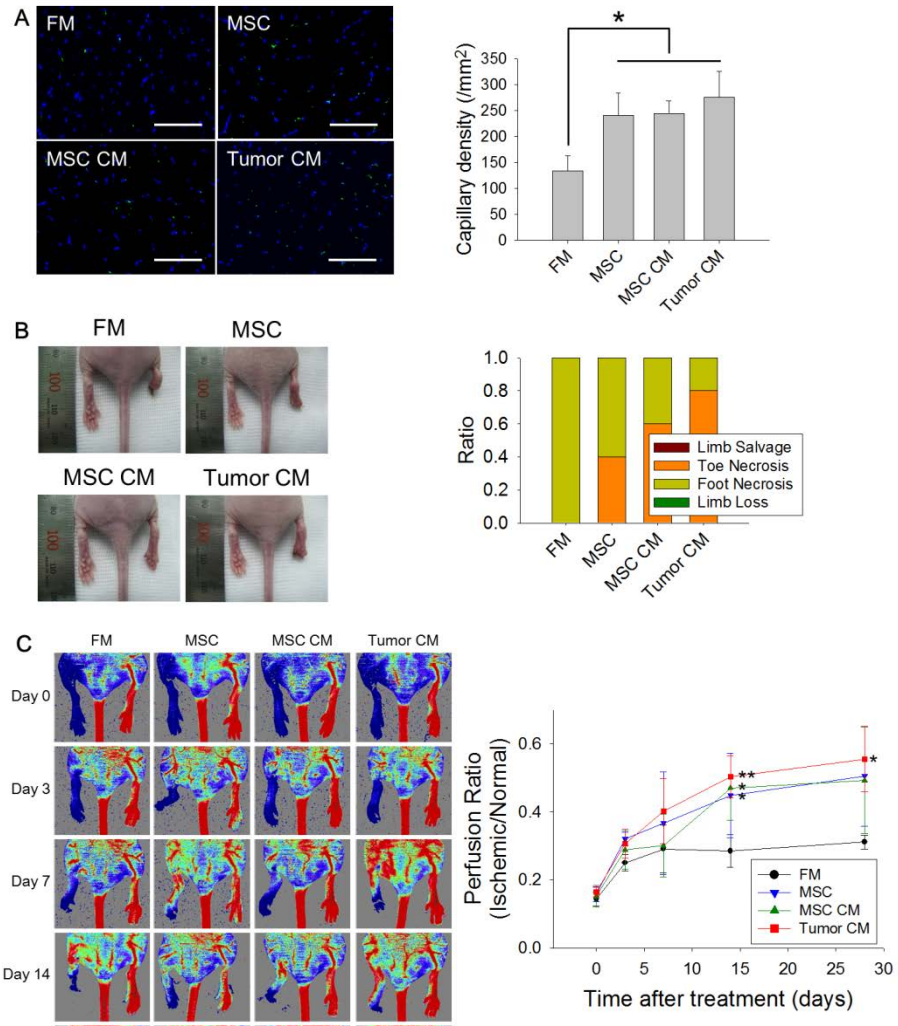
A
FM
MSC
MSC CM
Tumor CM
Capillary density (/mm2)
350
300
250
200
150
100
50
0
*
FM
MSC
MSC CM
Tumor CM
B
FM
MSC
MSC CM
Tumor CM
Ratio
1.0
0.8
0.6
0.4
0.2
0.0
Limb Salvage
Toe Necrosis
Foot Necrosis
Limb Loss
FM
MSC
MSC CM
Tumor CM
C
FM
MSC
MSC CM
Tumor CM
Day 0
Day 3
Day 7
Day 14
Day 28
Perfusion Ratio (Ischemic/Normal)
0.6
0.4
0.2
0.0
**
**
*
*
FM
MSC
MSC CM
Tumor CM
0
5
10
15
20
25
30
Time after treatment (days)

Figure 3.5. The treatment of mouse ischemic limbs with the injection of fresh medium (FM), MSCs, MSC CM, or HT1080 CM. (A) HT1080 CM was diluted with DMEM so that HT1080 CM and MSC CM had the same cell number basis. CD31-positive capillaries in the ischemic region after 28 days of treatment were stained with mouse CD31 antibody (light green). Blue indicates nuclei stained with DAPI (Bars = 100 μm, $*P < 0.05$). (B) Representative photographs of ischemic limbs 28 days after treatment. Limb salvage, toe necrosis, foot necrosis, and limb loss of each group were evaluated (n = 5 animals per group). (C) Representative laser Doppler images showing blood perfusion in the ischemic limbs on day 28. Blood perfusion of the ischemic limbs was monitored for 28 days. The quantitative data are mean ± SD of 5 animals per group ($*P < 0.05$ versus FM, $**P < 0.01$ versus FM).

3.2.7. Ischemic limb salvage by CM injection

The therapeutic potential of HT1080 CM was evaluated by physiological observation of the ischemic limbs (n=5 mice per group) 28 days after treatment (Figure 3.5.B). All of the mice that were treated with FM underwent foot necrosis. In contrast, the mice treated with HT1080 CM showed mild necrotic damage in the ischemic limbs. The majority (4 mice) of the mice treated with HT1080 CM underwent toe necrosis and the remaining fraction (1 mouse) of the mice underwent foot necrosis. Treatment with MSC CM and MSCs also attenuated ischemic damage compared with treatment using FM. Toe necrosis was observed in three of the mice treated with MSC CM and two of the mice treated with MSCs. Foot necrosis was observed in two of the mice treated with MSC CM and three of the mice treated with MSCs.

3.2.8. Blood perfusion in the ischemic limbs by CM injection

The Laser Doppler perfusion imaging analysis revealed that the blood perfusion in the ischemic limbs was significantly improved in the Tumor CM group compared with the FM group at day 14 and 28 (Figure 3.5.C). No significant difference in the perfusion ratio was observed among the Tumor CM, MSC CM and MSC groups at days 14 and 28.

3.3. Discussion

The therapeutic efficacy of stem cell-based therapy mainly results from the paracrine effects of the implanted stem cells [18, 21]. Therefore, the injection of stem cell CM may represent an alternative method for the stem cell implantation therapy. Stem cell CM contained various cytokines and growth factors [16]. Among the cytokines or growth factors, IL-6[22, 54], IL-8[23], MCP-1[63], bFGF[17, 18], HGF[17], or VEGF[17, 18, 22] have been reported to play an important role in revascularization of the ischemic tissue in MSC CM injection therapy. Indeed, these cytokines existed within detectable range of the antibody array analysis in both the CMs (Figure 3.3.). In addition, GM-CSF and PLGF that were secreted more from HT1080 cells than from MSCs have been proved to contribute vascularization in ischemic disease animal models [63-65]. Indeed, GM-CSF contributed to the ability of the HT1080 CM to enhance HUVEC proliferation, along with VEGF (Figure 3.4.). Collectively, we deduced these cytokines or angiogenic factors were responsible for the therapeutic outcome of the CM injection.

The low concentration of angiogenic factors in CM obtained from stem cell cultures, which mainly resulted from low cell density in conventional mono-layered cell cultures, could attenuate the translational application of stem cell CM therapy for ischemic disease treatment [40]. To elevate the angiogenic

factor concentrations of CM obtained from stem cell cultures, a three-dimensional (3D) cell culture method, which enables a high-density cell culture, has been suggested [40]. Unlike MSCs and ASCs, HT1080 cells do not require 3D cell culture for high-density cell culture because HT1080 cells can grow in multi-layers. After 7 days of 2D culture, the density of HT1080 cells reached 3.4×10^5 cells/cm^2 or 2.5×10^6 cells/ml (Figure 3.1.A), which is much higher than that of MSCs (1.8×10^4 cells/cm^2 or 1.3×10^5 cells/ml (Figure 3.1.A)). The HT1080 cell density (2.5×10^6 cells/ml) in 2D culture is even much higher than the ASC density (1.2×10^6 cells/ml) in 3D bioreactors in a previous study [40]. Indeed, the concentrations of pro-angiogenic factors, such as angiogenin, GM-CSF, PDGF-AA, and PLGF, were higher in HT1080 CM compared with MSC CM (Figure 3.3.). In addition, a much faster growth rate of HT1080 cells compared with MSCs (Figure 3.1.A) would be advantageous to produce CM on a large scale.

HT1080 cells potentially could be a stable cell source for the CM production since the HT1080 cell line can expand indefinitely *in vitro*. In contrast, MSCs undergo senescence during *in vitro* expansion [66]. Moreover, previous studies have reported that the VEGF secretion of the MSCs decreased[67] and the gene expression patterns of the MSCs changed[68] with increasing passage numbers, which may cause variations in CMs obtained from MSC cultures.

Although HT1080 cells have advantages over MSCs for producing therapeutic CM, clinical application of HT1080 CM has obstacles to overcome. Some ingredients of the culture media, such as 4-(2-hydroxyethyl)-1-piperazineethanesulfonic acid (HEPES), phenol red, and bovine serum, might be harmful [17]. Moreover, the risk of tumorigenesis by HT1080 CM injection has to be examined because the HT1080 cell itself is tumorigenic. In the present study, to reduce the risk of tumorigenesis by HT1080 cells, HT1080 CM was centrifuged and filtered through 0.2 μm filters to completely eliminate HT1080 cells. Accordingly, we did not observe tumor tissue in the ischemic limbs treated with HT1080 CM. However, the risk of tumorigenesis still remains one of the major challenges in the clinical application of tumor cell CM. Cancer cell exosomes and nano-vesicles containing mRNA, microRNA, and proteins showed pro-tumorigenic properties through delivering tumor-associated genetic information or proteins [6, 69]. Recently, Melo et al. reported that exosomes derived from the cells or sera of the patients with breast cancer stimulated tumorigenesis of non-tumorigenic immortal cells [70]. Therefore, for the clinical application of tumor cell CM, it is necessary to understand the effects of tumor cell CM on tumorigenesis and to control the risk of tumorigenesis.

Chapter 4.

Cutaneous wound healing via induction of angiogenesis by using an organic photovoltaic patch

4.1. Introduction

Wound healing is a complex process associated with various types of cells, cytokines, and growth factors. Appropriate regulation of immune reaction and therapeutic manipulation of skin cell behaviors are crucial for the treatment of recalcitrant wound, acceleration of wound healing, and minimization of the scar tissues. Among a series of endogenous healing mechanisms involved in wound repair, endogenous electric field (EF) ranging from 40 mV/mm to 200mV/mm that is generated by the breakage of transepithelial potential at the wound region, has been known as one of regulators for wound healing [29]. EF stimulates the behaviors of not only the skin cells but also the immune cells that participate in wound healing process by directing and enhancing migration of neutrophils [71, 72], keratinocytes [71, 73, 74], and fibroblasts [71, 75, 76]. Also, a number of previous studies showed that EF could upregulate protein synthesis by the fibroblasts [77, 78].

To better elucidate the therapeutic effect of EF and improve the wound repair process, researchers have applied exogenous electric stimulation on wound healing [79, 80]. Even though the previous researches regarding animal studies and clinical trials have reported that the exogenous electric stimulation was effective for wound healing [30, 81], most of these studies utilized large-sized devices to deliver electric stimulation on the injury site and required

hospitalization of the patients. Therefore, the development of a wearable device that can deliver electric stimulation at the wound site can minimize the inconvenience of patient hospitalization and allow more patient-friendly clinical application of electric stimulation therapy for wound healing. Additionally, unlike current wearable-sized wound dressings or dermal patches that only focus on minimizing tissue infections and rehydrating the wound sites [35], a wearable electric stimulation device can exert therapeutically-approved EF and actively augment the regenerative potential of the cells associated with wound repair.

The wearable electric stimulation device should be a self-powered system and among various energy harvesting concepts, the photovoltaic self-powering is the most suitable approach because continuous EF stimulation is necessary for better skin healing. Thus, we introduce here a wearable organic photovoltaic patch (OPP) for electrically stimulated wound healing therapy. Previous studies showed that continuous direct current ranging between 200 ~ 800 μA have positive outcome for the treatments of chronic wound [79]. OPP can generate current in a hundreds of μA scale or electric field (40 ~ 200 mV/mm) that are appropriate scale for cutaneous wound healing. Considering the commercialization of the organic photovoltaic patch, we choose a conventional organic solar cell based on poly(3-hexylthiophene) (P3HT) and the phenyl-C_{61}-butyric acid methyl ester (PCBM) bulk heterojunction as a

wearable and disposable EF generator because organic solar cell is mechanically flexible, biocompatible on skin and mass-producible with low cost process [38, 82].

Our patch consists of two parts; one is an organic solar cell and the other is a patch with outside-inside pair electrodes adjustable to the geometry of a wound. The solar cell and the electrodes of the patch are electrically connected, and all parts are integrated and packaged to be a single, wearable OPP. The outside electrode of patch is designed to cover whole wound area and the inside electrode is located the center of the injury area, thus EF generated by organic solar cell is averagely aligned along the direction of wound closing. Semi-permanent electrical stimulation under visible light illumination is possible in our patch; the continuous healing is expected as near as the patch is attached. Since the skin wounds can frequently occur in any of the body parts exposed to visible light, including hands, elbows, arms, knees, legs and back, the patch became a superior self-powered EF healing agent to commercialized normal healing patch.

In the present study, we tested the therapeutic efficacy of OPP in the back of mouse cutaneous wound models. OPPs were attached to the skin wounds of mice's backs so that the device could receive light energy from a LED lamp in a cage and convert it into electrical energy to deliver direct current at the wound site. The electrical energy that was applied on the wound through gold

electrode could amplify endogenous electric signal by enhancing ionic current in the wound. We first evaluated whether OPP successfully converted light energy into electrical energy, and exerted direct current suitable for wound healing at the wound area. Next, we investigated whether electrical stimulation from OPP managed to promote the regenerative activities of keratinocyte, fibroblasts and immune cells at the wound site by examining inflammation, re-epithelialization, proliferation, granulation, and tissue remodeling. Additionally, we assessed electrical stimulation-associated wound healing process in animal models by examining microvessel formation and wound size reduction.

4.2. Reuslts

4.2.1. Fabrication and characterization of wearable organic photovoltaic patch

Figure 4.1.A shows the schematic illustration of OPP. The patch was composed of two parts. One is organic solar cell part that generates electrical field. The patterned three organic solar cells were fabricated on one substrate as inverted structure type that has better stability in air and the devices were electrically connected in parallel to provide electrical stimulation to the wound. The other is electrode part of wound healing patch. The molded circle electrodes on PDMS substrate were combined with organic solar cell part. To evaluate the wound healing effect of the organic photovoltaic patch, the patches without solar cell or electrode were also fabricated (middle panel of Figure 4.1.A). The patches were applied to the back wounds of mice to test the healing effect (right panel of Figure 4.1.A). The patches were applied to the skin wounds of mice to test the healing effect as shown in Figure 4.1.B. Figure 4.1.C exhibits the experiment environment for the wounded mouse that wears the patch in cage with LED light (SFS Lights). Figure 4.1.D exhibits current voltage (I-V) curves of photovoltaic patch under various light angles considering mouse behaviors. Although open circuit voltage (Voc) and short circuit current (Isc) decreased as increasing the light angle due to reduced

light intensity, the actual output voltage and current under the light followed the tendency and maintained over 0.3 V and 100 μA. Applied voltage and current were calculated from the wound resistance (≈ 100 kΩ), that the patches deliver when attached on the wound (Table 4.1.). The applied voltage was similar with the Voc and the applied current was about 4 μA.

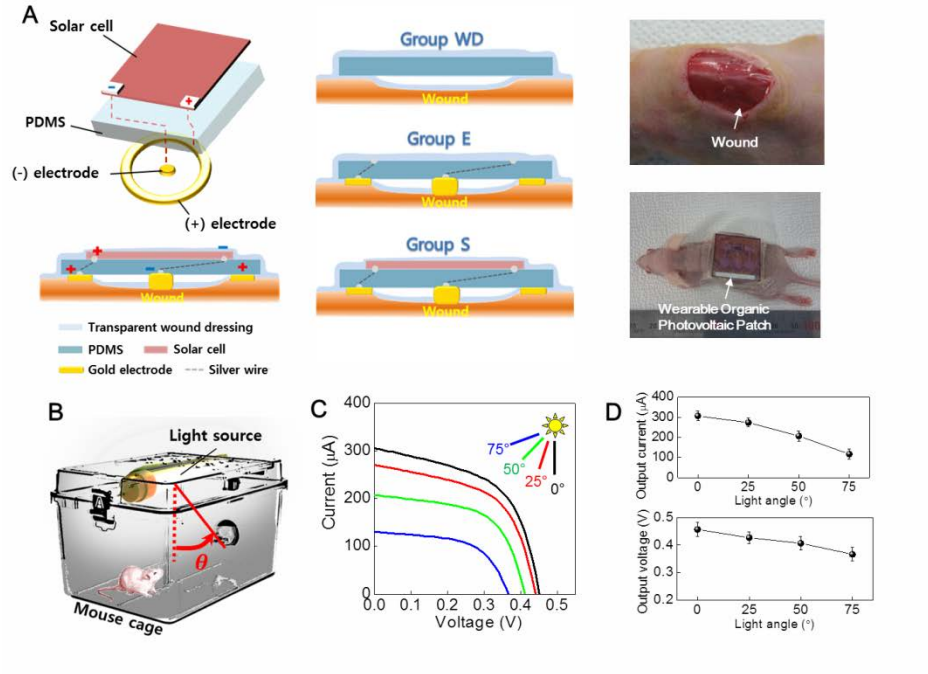

Figure 4.1. Treatment with a wearable organic photovoltaic patch (OPP). (A) Schematic illustration of manufacture of the organic photovoltaic patch and its application for mouse wound models. (B) Illustration of the experimental environment for the wounded mouse that wears the patch in the cage with LED light. (C) Photovoltaic capacity of the patch according to change of the light angle. (D) Graph about output current, output voltage, applied current and applied voltage of the patch according to change of the light angle.

Table 4.1. Applied current and voltage

Light angle (˚)	**Applied current (μA)**	**Applied voltage (V)**
0	4.80	0.45
25	4.80	0.44
50	4.20	0.41
75	3.75	0.36

4.2.2. Accelerated wound closer by the OPP

To evaluate the therapeutic effect of OPP in mouse models, three groups including wound dressing (WD, wound site treated with only PDMS substrate), electrode only (E, wound site treated with the electrode part that has no solar cells to generate electrical stimulation) and OPP (S, wound site treated with OPP that generates electrical stimulation) were used *in vivo*. All groups were dressed with transparent Tegaderm film (Tegaderm^{TM}, 3M Health Care, St. Paul, MN, USA) to minimize tissue infections and rehydrate wound [35]. Digital photographs of the wound region were taken at day 0, 3, 6, 9, and 12 days after each treatment and the relative wound area at each time point was expressed as the percentage relative to the original wound size (Figure 4.2.A). WD group, which had no treatment after wound induction, served as the negative control group. At days 6 and 9, all three groups showed significant wound size reduction compared to day 0, but no statistically significant defect reduction was observed between any two groups. However, at day 12, the S group had a greatly smaller wound area compared with the other groups (Figure 4.2.A). Groups treated with electrodes only but no solar cells exhibited no notable wound reduction compared with the WD group. Masson's trichrome staining further showed that more collagen deposition

were observed in the E group compared with the WD and E groups (Figure 4.2.B).

Next, a histological evaluation of intersubcutenous distance was utilized to quantitatively assess wound closure. Twelve days after the treatments, intersubcutaneous distance in the S group was significantly shorter than the other groups (Figure 4.2.C). Such decrease in intersubcutaneous distance was further accompanied with the enhanced regeneration of basal layer (expression of laminin, Figure 4.2.D and 4.2.E) and epidermis layer (expression of involucrin, Figure 4.2.D and 4.2.E). Immunohistochemical staining of laminin, a biomarker for skin basal layer, showed significantly enhanced protein expression of laminin in the groups treated with OPP, compared to the other groups (Figure 4.2.D, upper panel). Staining of involucrin, a representative biomarker for skin epidermis layer, also exhibited great increase in the S group compared to the WD or E groups (Figure 4.2.D, lower panel). Similarly, western blot analysis regarding these biomarkers showed OPP treatment significantly promoted basal and epidermis layer regeneration (Figure 4.2.E). Overall, these results showed that OPP-derived electrical stimulation treatment can expedite the collagen synthesis at the wound lesion and better regenerate tissue basal and epidermis layer to reduce the wound defect area.

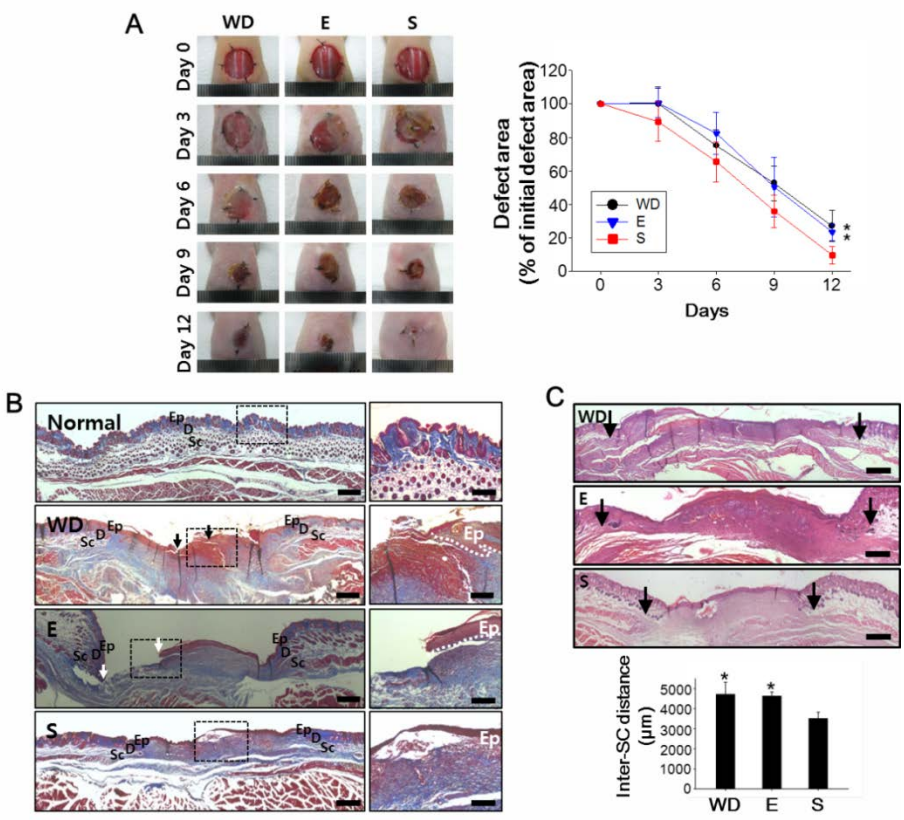
A
WD
E
S
Day 0
Day 3
Day 6
Day 9
Day 12
Defect area
(% of initial defect area)
120
100
80
60
40
20
0
WD
E
S
0
3
6
9
12
Days
B
Normal
Ep
D
Sc
WD
E
S
C
WDI
E
S
Inter-SC distance
(μm)
5000
4000
3000
2000
1000
0
WD
E
S

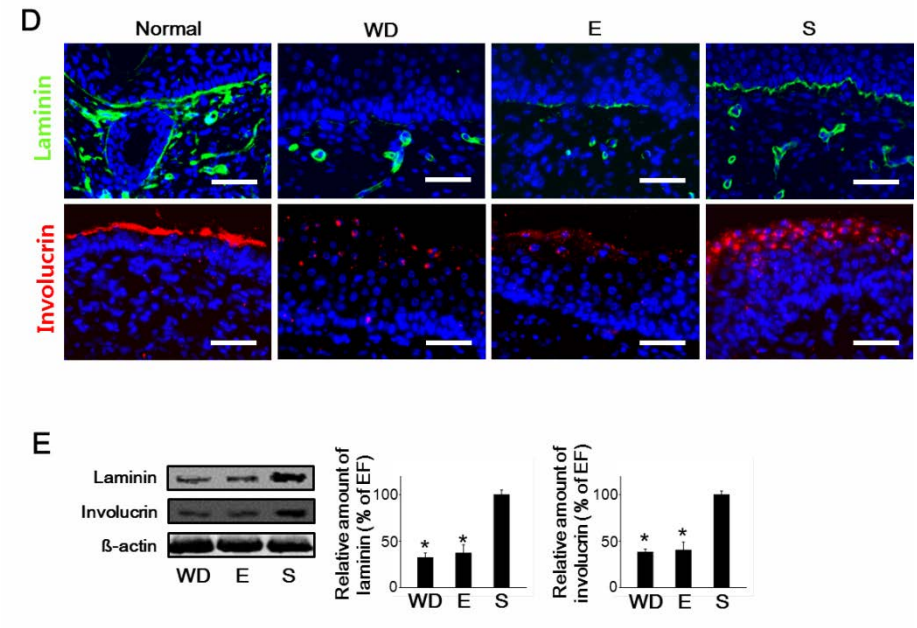

Figure 4.2. Accelerated wound healing by treatment with the OPP. (A) Representative photographs and quantification of the skin wound closure 0, 3, 6, 9, and 12 days after each treatment. n = 8, ** $p < 0.01$ compared to S. (B) Masson's trichrome-stained sections of the wound healing regions 12 days after each treatment. Bars indicate = 500 μm (left pannel), 200 μm (right pannel). (C) Hematoxylin and eosin stained sections of the wound healing regions 12 days after the treatments, and the intersubcutaneous distance measurements. Arrows indicate the starting and end point of intersubcutaneous distance. * $p < 0.01$ compared to S. (D) Immunohstochemical staining for laminin (green) in the basal layer (left) and invorlucrin (red) in epidermis at the wound healing region 12 days after

treatments Bars indicate = 50 μm. (E) Protein expression and quantification of laminin and invorlucrin at the wound beds 12 days after the treatments evaluated by western blot analysis * $p < 0.05$ compared to the S group.

4.2.3. Enhanced wound healing process by the OPP

We evaluated the step-by-step wound healing process enhanced by the OPP treatment, and assessed whether electrical stimulation generated by the OPP treatment promoted each phase of wound repair process, namely the inflammatory phase, proliferation phase, and remodeling phase (Figure 4.3.A). Inflammation, cell proliferation, and tissue remodeling phases for wound healing were assessed using western blot analysis at 3, 9, and 12 days after the treatments, respectively (Figure 4.3.B-D). During the inflammatory phase of wound repair, a significant upregulation of an inflammatory macrophage marker, CD68, was observed in the S group compared with the other groups (Figure 4.3.B). Moreover, vascular endothelial growth factor (VEGF) was also greatly enhanced with the OPP treatment in this phase (Figure 4.3.B). VEGF, which can be derived from neutrophils and macrophages, can also contribute to wound healing by recruiting inflammatory macrophages to the wound region [83].

At day 9, tissue samples were retrieved and analyzed to evaluate active proliferation phase at the wound site. As shown in Figure 4.3.A, proliferative phase consists of granulation tissue formation, cell proliferation, extracellular matrix (ECM) synthesis, angiogenesis and re-epithelialization. During this phase, a significant upregulation of cell proliferating marker, PCNA, was

observed (Figure 4.3.C), in accordance with the results of a previous study [84]. Additionally, protein expression of collagen type III (COL III), transforming growth factor-beta (TGF-β), an endothelial cell marker (CD99), integrin alpha-V subunit (Iα5), and matrix metalloproteinase 2 (MMP2) greatly increased in the S group compared with the other groups (Figure 4.3.C). After the inflammatory phase, significant angiogenesis is required at the wound region to expedite granulation tissue formation and ECM synthesis [85, 86]. Among various types of proteins, TGF-β, CD99, and Iα5 have been previously shown crucial in vascular development and therapeutic angiogenesis [85-87]. MMP2, which plays a crucial role in break-down and re-establishment of ECM in tissue remodeling, has been known to be highly expressed during the granulation tissue formation [88], thus a significant upregulation of MMP2 in the S group (Figure 4.3.C) further demonstrated that more granulation tissue formation was undergoing in the groups treated with OPP compared with the other groups. Enhanced protein expression of COL III (Figure 4.3.C), which is important for basement membrane regeneration in the wound repair process [85], also denotes the therapeutic efficacy of electrical stimulation by the OPP in cutaneous wound healing.

During tissue remodeling phase, we observed notable increase in fibronectin, collagen type IV (COL IV), and collage type I (COL I) in the S group compared with the other groups (Figure 4.3.D). Fibronectin plays a

crucial role in capillary formation, thus participating in granulation tissue re-organization and tissue basement membrane formation during wound healing [89]. Moreover, enhanced expression of COL IV in the S group (Figure 4.3.D) may also improve keratinocyte proliferation and expedite membrane reconstitution for wound healing, as noted by the results of a previous study [90]. Additionally, increase in COL I protein expression (Figure 4.3.D) demonstrates that OPP treatment better accelerated wound maturation compared to the other groups [85]. Overall, these data suggest that OPP participated in every stage of wound healing process by regulating wound inflammation, by accelerating cell proliferation and granulation tissue formation, and by completing tissue remodeling.

To further visualize therapeutic angiogenesis at the wound region by OPP treatment, immunofluorescent staining for microvessel biomarker (Von Willebrand factor, vWF) was performed. Twelve days after the treatments, groups treated with OPP showed enhanced microvessel formation at the wound region compared with the other groups (Figure 4.3.E).

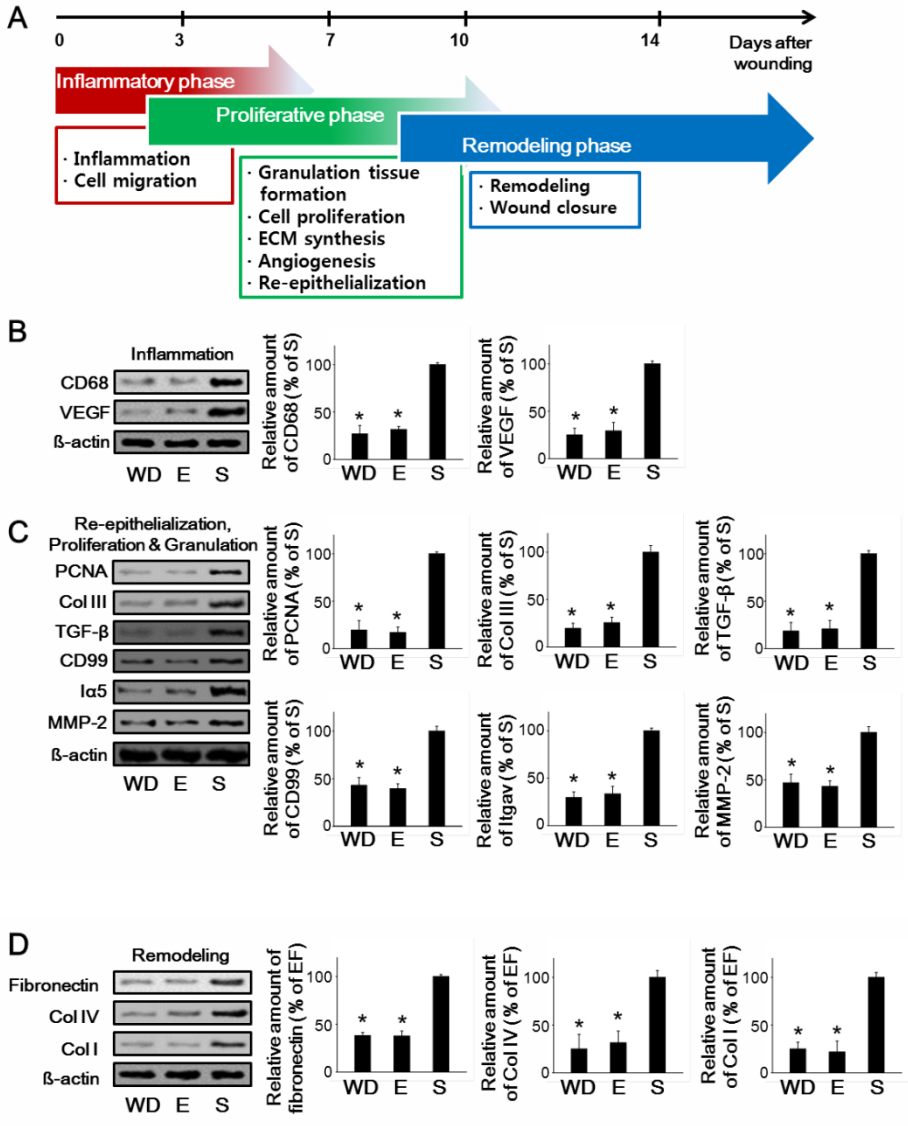
A
0
3
7
10
14
Days after wounding
Inflammatory phase
Proliferative phase
Remodeling phase
· Inflammation
· Cell migration
· Granulation tissue formation
· Cell proliferation
· ECM synthesis
· Angiogenesis
· Re-epithelialization
· Remodeling
· Wound closure
B
Inflammation
CD68
VEGF
ß-actin
WD E S
Relative amount of CD68 (% of S)
Relative amount of VEGF (% of S)
C
Re-epithelialization, Proliferation & Granulation
PCNA
Col III
TGF-β
CD99
Iα5
MMP-2
ß-actin
Relative amount of PCNA (% of S)
Relative amount of Col III (% of S)
Relative amount of TGF-β (% of S)
Relative amount of CD99 (% of S)
Relative amount of Itgav (% of S)
Relative amount of MMP-2 (% of S)
D
Remodeling
Fibronectin
Col IV
Col I
ß-actin
Relative amount of fibronectin (% of EF)
Relative amount of Col IV (% of EF)
Relative amount of Col I (% of EF)

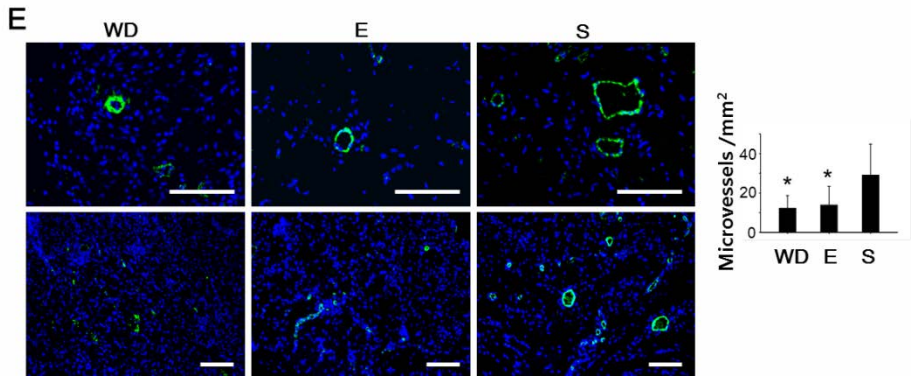

Figure 4.3. Wound healing process enhanced by treatment with the OPP. (A) Schematic illustration of the wound healing process. (B) Expression and quantification of the proteins related to the inflammatory phase of the wound healing process. (C) Expression and quantification of the proteins contributing to the proliferative phase of the wound healing process. (D) Expression and quantification of the proteins involved in remodeling phase of the wound healing process. (E) Immunohistochemical staining and quantification of vWF-positive microvessels at the wound healing region 12 days after the treatments. Bars indicate 100 μm. * $p < 0.05$ compared to the S group in A-D.

4.2.4. Effect of electrical stimulation of dermal fibroblast

To elucidate the effect of electrical stimulation by OPP, fibroblasts were cultured on electric chamber and exposed electrical stimulation (70 mV/mm). Scratch was made on fibroblast monolayer in electric chamber and the cells were exposed electrical stimulation for 6hr. Healing area was significantly increased in the cells exposed electrical stimulation compared to control cells (Figure 4.3.A). After further culture of the cells without electric stimulation for 18 hr, gene expression of the cells was analyzed by qRT-PCR. Relative Ki67 and PCNA gene expression was significantly increased by electrical stimulation (Figure 4.4.B), suggesting the enhanced proliferation of fibroblasts. Also, fibronectin and COL III gene expression was upregulated in the electrically stimulated fibroblasts (Figure 4.4.C).

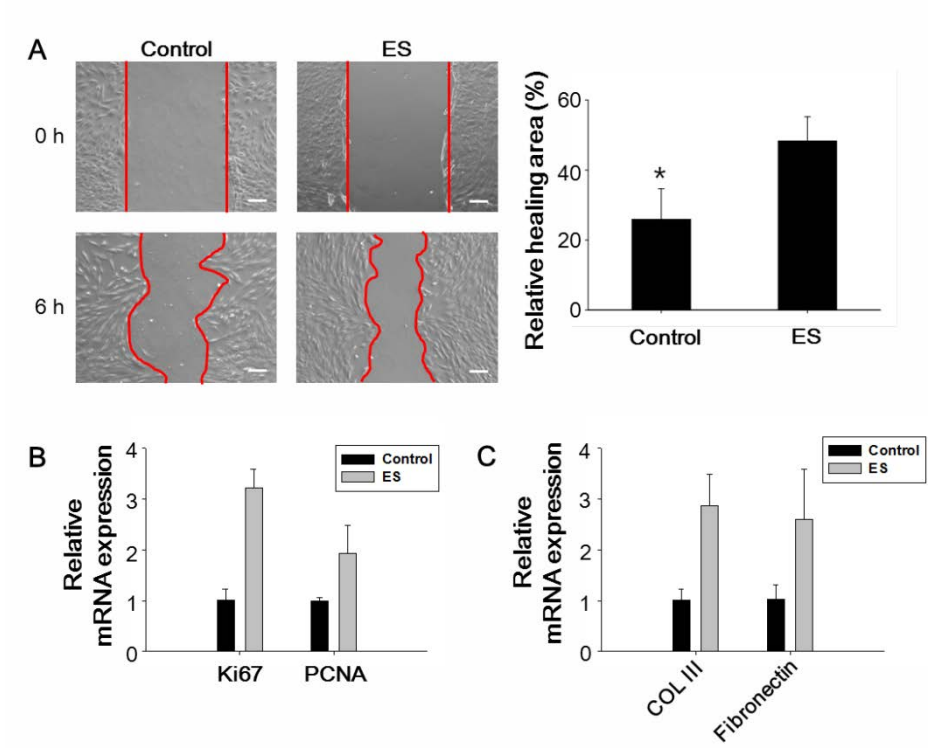

Figure 4.4 Effects of electrical stimulation on dermal fibroblast *in vitro*. (A) Effect of electrical stimulation on fibroblast migration. (B) Proliferation associated gene expression and (C) extracellular matrix gene expression after electrical stimulation. Bars indicate 200 μm. * $p < 0.05$ compared to the ES group in A-C.

4.3. Discussion

In the present study, we introduced the OPP for delivering electrical stimulation on skin wounds. The applied current was about 4 μA that are much smaller than the current (200 ~ 800 μA) that have been proved effective for chronic wound treatment [79]. Recently, Sara Ud-Din reported that electric stimulation of degenerative wave form delivering 4 μA of current had therapeutic outcome for cutaneous wound model [91], which support the validity of using our patch for cutaneous wound healing. The applied voltage of the OPP was from 0.36 V to 0.45 V according to change of light angle (Table 4.1.). Strength of electric field corresponding to the applied voltage was 65 ~ 82 mV/mm, that are similar to strength of endogenous wound electric field. We confirmed that the 70 mV/mm of electric field successfully enhanced regenerative activities of dermal fibroblasts *in vitro* (Figure 4.4), though there were differences between *in vitro* and *in vivo* study. Since resistivity of culture medium is lower than that of skin tissue [29, 39], current density in the medium was quite larger than in the skin wound when equal strength of electric field was formed. Moreover, we could not replicate the effect of exogenous electric field interaction with the endogenous wound electric field *in vivo*. Thus we tested therapeutic efficacy of exogenous electric stimulation by the OPP in the mouse cutaneous wound model. Indeed, wound

closure was accelerated in OPP treated mice (Figure 4.2.A). Also, collagen deposition was increased in OPP treated mice compared with the WD and E groups (Figure 4.2.B). Formation and deposition of collagen fibers are particularly important in wound repair, because collagen is critical for granulation tissue organization and tissue membrane regeneration during the wound healing process [85]. Additionally, more collagen observed in the S group demonstrates that electrical stimulation generated by OPP may have affected collagen synthesis by the fibroblasts, as observed in a previous study [92]. OPP treatment also enhanced re-epithelialization of the epidermis layer at the wound region, while the WD or E group showed breakdown of epidermis layer (Figure 4.2.B). These data demonstrated that the electric stimulation by the OPP was effective for cutaneous wound heling.

Further study about the wound healing phase elucidated effects of the electrical stimulation in healing process. In the inflammatory phase, vascular endothelial growth factor (VEGF) was enhanced in the S group compared with the WD or E group (Figure 4.3.B). VEGF is known to be majorly upregulated during the inflammation phase [93], hence enhanced macrophage expression along with VEGF during the initial phase of wound healing process seemed reasonable. Recruitment of inflammatory macrophages is particularly important, because newly recruited macrophages can secrete a variety of cytokines involved in angiogenesis [94], clearance of cell debris

from the wound site [95], fibroblast proliferation and collagen synthesis. Also, treatment with the OPP increased microvessel density in the wound site (Figure 4.3.E). OPP does not utilize exogenous drug delivery, hence, this result demonstrates that OPP induced host-inductive blood vessel formation through enhanced VEGF (Figure 4.3.B) or fibronectin (Figure 4.3.D) expression [83, 89, 94]. Therefore, these results collectively propose that OPP treatment may serve as a more patient-friendly therapeutics for wound healing.

Chapter 5.

Conclusion

This study presents the novel methods to treat hindlimb ischemia and cutaneous wound by inducing angiogenesis. In chapter 3, conditioned medium collected from human fibrosarcoma HT1080 cell culture was used to induce angiogenesis. Therapeutic potential of HT1080 CM was demonstrated in mouse hindlimb ischemia models. *In vitro* growth in multilayers, fast growth rate, and secretion of angiogenic factors of HT1080 cells were advantages to produce a therapeutically effective CM for ischemic disease treatment. In chapter 4, we fabricated a wearable organic photovoltaic patch for treatment of cutaneous wound. Our patch was applied to the wounds of mouse, and deliverd electrical signal on wound. The deliverd electric signal together with the endogenous wound electric field stimulated the cells participating in wound healing process. Subsequently, enhanced growth factor secretion, ECM protein synthesis, cell proliferation, and angiogenesis in the wound resulted in aceleralation of wound closure and skin regeneration.

References

[1] Liew A, O'Brien T. Therapeutic potential for mesenchymal stem cell transplantation in critical limb ischemia. Stem Cell Res Ther. 2012;3:1.

[2] Perin EC, Silva GV. Cell-Based Therapy for Chronic Ischemic Heart Disease—A Clinical Perspective. Cardiovasc Ther. 2011;29:211-7.

[3] Karantalis V, Balkan W, Schulman IH, Hatzistergos KE, Hare JM. Cell-based therapy for prevention and reversal of myocardial remodeling. American Journal of Physiology-Heart and Circulatory Physiology. 2012;303:H256-H70.

[4] Wu KH, Mo XM, Han ZC, Zhou B. Stem cell engraftment and survival in the ischemic heart. The Annals of thoracic surgery. 2011;92:1917-25.

[5] Segers VF, Lee RT. Stem-cell therapy for cardiac disease. Nature. 2008;451:937-42.

[6] Peinado H, Aleckovic M, Lavotshkin S, Matei I, Costa-Silva B, Moreno-Bueno G, et al. Melanoma exosomes educate bone marrow progenitor cells toward a pro-metastatic phenotype through MET. Nature medicine. 2012;18:883-91.

[7] Tang J-M, Luo B, Xiao J-h, Lv Y-x, Li X-l, Zhao J-h, et al. VEGF-A promotes cardiac stem cell engraftment and myocardial repair in the infarcted heart. Int J Cardiol. 2015;183:221-31.

[8] Babensee JE, McIntire LV, Mikos AG. Growth factor delivery for tissue engineering. Pharm Res. 2000;17:497-504.

[9] Mangi AA, Noiseux N, Kong D, He H, Rezvani M, Ingwall JS, et al. Mesenchymal stem cells modified with Akt prevent remodeling and restore performance of infarcted hearts. Nat Med. 2003;9:1195-201.

[10] Fischer KM, Cottage CT, Wu W, Din S, Gude NA, Avitabile D, et al. Enhancement of myocardial regeneration through genetic engineering of cardiac progenitor cells expressing Pim-1 kinase. Circulation. 2009;120:2077-87.

[11] Tang YL, Tang Y, Zhang YC, Qian K, Shen L, Phillips MI. Improved graft mesenchymal stem cell survival in ischemic heart with a hypoxia-regulated heme oxygenase-1 vector. J Am Coll Cardiol. 2005;46:1339-50.

[12] Sekine H, Shimizu T, Dobashi I, Matsuura K, Hagiwara N, Takahashi M, et al. Cardiac cell sheet transplantation improves damaged heart function via superior cell survival in comparison with dissociated cell injection. Tissue Engineering Part A. 2011;17:2973-80.

[13] Ishii M, Shibata R, Numaguchi Y, Kito T, Suzuki H, Shimizu K, et al. Enhanced angiogenesis by transplantation of mesenchymal stem cell sheet created by a novel magnetic tissue engineering method. Atertio Thromb Vasc Biol. 2011;31:2210-5.

[14] Bhang SH, Cho SW, La WG, Lee TJ, Yang HS, Sun AY, et al.

Angiogenesis in ischemic tissue produced by spheroid grafting of human adipose-derived stromal cells. Biomaterials. 2011;32:2734-47.

[15] Bhang SH, Lee S, Shin J-Y, Lee T-J, Kim B-S. Transplantation of cord blood mesenchymal stem cells as spheroids enhances vascularization. Tissue engineering Part A. 2012;18:2138-47.

[16] Caplan AI, Dennis JE. Mesenchymal stem cells as trophic mediators. Journal of cellular biochemistry. 2006;98:1076-84.

[17] Bhang SH, Lee S, Shin JY, Lee TJ, Jang HK, Kim BS. Efficacious and clinically relevant conditioned medium of human adipose-derived stem cells for therapeutic angiogenesis. Mol Ther. 2014;22:862-72.

[18] Kinnaird T, Stabile E, Burnett MS, Shou M, Lee CW, Barr S, et al. Local delivery of marrow-derived stromal cells augments collateral perfusion through paracrine mechanisms. Circulation. 2004;109:1543-9.

[19] Lee RH, Pulin AA, Seo MJ, Kota DJ, Ylostalo J, Larson BL, et al. Intravenous hMSCs improve myocardial infarction in mice because cells embolized in lung are activated to secrete the anti-inflammatory protein TSG-6. Cell stem cell. 2009;5:54-63.

[20] Ranganath SH, Levy O, Inamdar MS, Karp JM. Harnessing the mesenchymal stem cell secretome for the treatment of cardiovascular disease. Cell stem cell. 2012;10:244-58.

[21] Li Z, Guo J, Chang Q, Zhang A. Paracrine role for mesenchymal stem

cells in acute myocardial infarction. Biol Pharm Bull. 2009;32:1343-6.

[22] Kwon HM, Hur SM, Park KY, Kim CK, Kim YM, Kim HS, et al. Multiple paracrine factors secreted by mesenchymal stem cells contribute to angiogenesis. Vascular pharmacology. 2014;63:19-28.

[23] Kwon YW, Heo SC, Jeong GO, Yoon JW, Mo WM, Lee MJ, et al. Tumor necrosis factor-α-activated mesenchymal stem cells promote endothelial progenitor cell homing and angiogenesis. Biochimica et Biophysica Acta (BBA)-Molecular Basis of Disease. 2013;1832:2136-44.

[24] Reinke J, Sorg H. Wound repair and regeneration. Eur Surg Res. 2012;49:35-43.

[25] Baum CL, Arpey CJ. Normal cutaneous wound healing: clinical correlation with cellular and molecular events. Dermatol Surg. 2005;31:674-86.

[26] Clark RA. Fibrin and wound healing. Ann NY Acad Sci. 2001;936:355-67.

[27] Oberringer M, Meins C, Bubel M, Pohlemann T. In vitro wounding: effects of hypoxia and transforming growth factor β1 on proliferation, migration and myofibroblastic differentiation in an endothelial cell-fibroblast co-culture model. Journal of molecular histology. 2008;39:37-47.

[28] Nuccitelli R, Nuccitelli P, Ramlatchan S, Sanger R, Smith PJ. Imaging the electric field associated with mouse and human skin wounds. Wound

Repair Regen. 2008;16:432-41.

[29] Nuccitelli R. A role for endogenous electric fields in wound healing. Curr Top Dev Biol. 2003;58:1-26.

[30] Ramadan A, Elsaidy M, Zyada R. Effect of low-intensity direct current on the healing of chronic wounds: a literature review. J Wound Care. 2008;17:292-6.

[31] Kloth LC. Electrical stimulation technologies for wound healing. Adv Wound Care. 2014;3:81-90.

[32] Assimacopoulos D. Low intensity negative electric current in the treatment of ulcers of the leg due to chronic venous insufficiency: Preliminary report of three gases. The American Journal of Surgery. 1968;115:683-7.

[33] Gault WR, Gatens Jr P. Use of low intensity direct current in management of ischemic skin ulcers. Phys Ther. 1976;56:265-9.

[34] Ud-Din S, Bayat A. Electrical stimulation and cutaneous wound healing: A review of clinical evidence. Healthcare: Multidisciplinary Digital Publishing Institute; 2014. p. 445-67.

[35] Murphy PS, Evans GR. Advances in wound healing: a review of current wound healing products. Plastic surgery international. 2012;2012.

[36] Ishibashi H, Nakagawa K, Nakashima Y, Sueishi K. Conditioned media of carcinoma cells cultured in hypoxic microenvironment stimulate angiogenesis in vitro; relationship to basic fibroblast growth factor. Virchows

Archiv. 1995;425:561-8.

[37] Hung SC, Pochampally RR, Chen SC, Hsu SC, Prockop DJ. Angiogenic effects of human multipotent stromal cell conditioned medium activate the PI3K-Akt pathway in hypoxic endothelial cells to inhibit apoptosis, increase survival, and stimulate angiogenesis. Stem Cells. 2007;25:2363-70.

[38] Oh JY, Lee TI, Myoung JM, Jeong U, Baik HK. Coating on a cold substrate largely enhances power conversion efficiency of the bulk heterojunction solar cell. Macromol Rapid Commun. 2011;32:1066-71.

[39] Chao P-HG, Roy R, Mauck RL, Liu W, Valhmu WB, Hung CT. Chondrocyte translocation response to direct current electric fields. J Biomech Eng. 2000;122:261-7.

[40] Bhang SH, Lee S, Shin J-Y, Lee T-J, Jang H-K, Kim B-S. Efficacious and clinically relevant conditioned medium of human adipose-derived stem cells for therapeutic angiogenesis. Mol Ther. 2014;22:862-72.

[41] Amado LC, Saliaris AP, Schuleri KH, John MS, Xie J-S, Cattaneo S, et al. Cardiac repair with intramyocardial injection of allogeneic mesenchymal stem cells after myocardial infarction. Proc Natl Acad Sci U S A. 2005;102:11474-9.

[42] Bhang SH, Cho S-W, La W-G, Lee T-J, Yang HS, Sun A-Y, et al. Angiogenesis in ischemic tissue produced by spheroid grafting of human adipose-derived stromal cells. Biomaterials. 2011;32:2734-47.

[43] Kalka C, Masuda H, Takahashi T, Kalka-Moll WM, Silver M, Kearney M, et al. Transplantation of ex vivo expanded endothelial progenitor cells for therapeutic neovascularization. Proceedings of the National Academy of Sciences. 2000;97:3422-7.

[44] Song H, Song B-W, Cha M-J, Choi I-G, Hwang K-C. Modification of mesenchymal stem cells for cardiac regeneration. Expert Opin Biol Ther. 2010;10:309-19.

[45] Menasche P. Stem cells for clinical use in cardiovascular medicine: current limitations and future perspectives. Thrombosis and haemostasis. 2005;94:697-701.

[46] Kinnaird T, Stabile E, Burnett MS, Lee CW, Barr S, Fuchs S, et al. Marrow-derived stromal cells express genes encoding a broad spectrum of arteriogenic cytokines and promote in vitro and in vivo arteriogenesis through paracrine mechanisms. Circulation research. 2004;94:678-85.

[47] Di Santo S, Yang Z, von Ballmoos MW, Voelzmann J, Diehm N, Baumgartner I, et al. Novel cell-free strategy for therapeutic angiogenesis: in vitro generated conditioned medium can replace progenitor cell transplantation. PLoS One. 2009;4:e5643.

[48] Kim JY, Song SH, Kim KL, Ko JJ, Im JE, Yie SW, et al. Human cord blood-derived endothelial progenitor cells and their conditioned media exhibit therapeutic equivalence for diabetic wound healing. Cell transplantation.

2010;19:1635-44.

[49] Shen C, Li L, Feng T, Li J, Yu M, Lu Q, et al. Dental pulp stem cells derived conditioned medium promotes angiogenesis in hindlimb ischemia. Tissue Engineering and Regenerative Medicine. 2015;12:59-68.

[50] Bergers G, Benjamin LE. Tumorigenesis and the angiogenic switch. Nature reviews Cancer. 2003;3:401-10.

[51] Kerbel RS. Tumor angiogenesis. New Engl J Med. 2008;358:2039-49.

[52] Katanasaka Y, Asai T, Naitou H, Ohashi N, Oku N. Proteomic characterization of angiogenic endothelial cells stimulated with cancer cell-conditioned medium. Biol Pharm Bull. 2007;30:2300-7.

[53] Kwon HM, Hur S-M, Park K-Y, Kim C-K, Kim Y-M, Kim H-S, et al. Multiple paracrine factors secreted by mesenchymal stem cells contribute to angiogenesis. Vascul Pharmacol. 2014;63:19-28.

[54] Simons D, Grieb G, Hristov M, Pallua N, Weber C, Bernhagen J, et al. Hypoxia-induced endothelial secretion of macrophage migration inhibitory factor and role in endothelial progenitor cell recruitment. J Cell Mol Med. 2011;15:668-78.

[55] Tello-Montoliu A, Patel J, Lip G. Angiogenin: a review of the pathophysiology and potential clinical applications. J Thromb Haemost. 2006;4:1864-74.

[56] Bussolino F, Ziche M, Wang JM, Alessi D, Morbidelli L, Cremona O, et

al. In vitro and in vivo activation of endothelial cells by colony-stimulating factors. The Journal of clinical investigation. 1991;87:986-95.

[57] Mehta VB, Besner GE. HB-EGF promotes angiogenesis in endothelial cells via PI3-kinase and MAPK signaling pathways. Growth factors. 2007;25:253-63.

[58] Awada HK, Johnson NR, Wang Y. Dual Delivery of Vascular Endothelial Growth Factor and Hepatocyte Growth Factor Coacervate Displays Strong Angiogenic Effects. Macromol Biosci. 2014;14:679-86.

[59] Gillis P, Savla U, Volpert OV, Jimenez B, Waters CM, Panos RJ, et al. Keratinocyte growth factor induces angiogenesis and protects endothelial barrier function. J Cell Sci. 1999;112:2049-57.

[60] Fiedler U, Augustin HG. Angiopoietins: a link between angiogenesis and inflammation. Trends Immunol. 2006;27:552-8.

[61] Sellke FW, Li J, Stamler A, Lopez JJ, Thomas KA, Simons M. Angiogenesis induced by acidic fibroblast growth factor as an alternative method of revascularization for chronic myocardial ischemia. Surgery. 1996;120:182-8.

[62] Ahrendt G, Chickering DE, Ranieri JP. Angiogenic growth factors: a review for tissue engineering. Tissue Eng. 1998;4:117-30.

[63] Luttun A, Tjwa M, Moons L, Wu Y, Angelillo-Scherrer A, Liao F, et al. Revascularization of ischemic tissues by PlGF treatment, and inhibition of

tumor angiogenesis, arthritis and atherosclerosis by anti-Flt1. Nat Med. 2002;8:831-40.

[64] Buschmann IR, Hoefer IE, van Royen N, Katzer E, Braun-Dulleaus R, Heil M, et al. GM-CSF: a strong arteriogenic factor acting by amplification of monocyte function. Atherosclerosis. 2001;159:343-56.

[65] Takahashi T, Kalka C, Masuda H, Chen D, Silver M, Kearney M, et al. Ischemia-and cytokine-induced mobilization of bone marrow-derived endothelial progenitor cells for neovascularization. Nat Med. 1999;5:434-8.

[66] Derubeis AR, Cancedda R. Bone marrow stromal cells (BMSCs) in bone engineering: limitations and recent advances. Ann Biomed Eng. 2004;32:160-5.

[67] Crisostomo PR, Wang M, Wairiuko GM, Morrell ED, Terrell AM, Seshadri P, et al. High passage number of stem cells adversely affects stem cell activation and myocardial protection. Shock. 2006;26:575-80.

[68] Wagner W, Horn P, Castoldi M, Diehlmann A, Bork S, Saffrich R, et al. Replicative senescence of mesenchymal stem cells: a continuous and organized process. PLoS One. 2008;3:e2213.

[69] Skog J, Wurdinger T, van Rijn S, Meijer DH, Gainche L, Sena-Esteves M, et al. Glioblastoma microvesicles transport RNA and proteins that promote tumour growth and provide diagnostic biomarkers. Nature cell biology. 2008;10:1470-6.

[70] Melo SA, Sugimoto H, O'Connell JT, Kato N, Villanueva A, Vidal A, et al. Cancer exosomes perform cell-independent microRNA biogenesis and promote tumorigenesis. Cancer cell. 2014;26:707-21.

[71] Zhao M, Song B, Pu J, Wada T, Reid B, Tai G, et al. Electrical signals control wound healing through phosphatidylinositol-3-OH kinase-γ and PTEN. Nature. 2006;442:457-60.

[72] Lin F, Baldessari F, Gyenge CC, Sato T, Chambers RD, Santiago JG, et al. Lymphocyte electrotaxis in vitro and in vivo. The Journal of Immunology. 2008;181:2465-71.

[73] Sheridan DM, Isseroff RR, Nuccitelli R. Imposition of a physiologic DC electric field alters the migratory response of human keratinocytes on extracellular matrix molecules. J Invest Dermatol. 1996;106:642-6.

[74] Nishimura KY, Isseroff RR, Nuccitelli R. Human keratinocytes migrate to the negative pole in direct current electric fields comparable to those measured in mammalian wounds. J Cell Sci. 1996;109:199-207.

[75] Guo A, Song B, Reid B, Gu Y, Forrester JV, Jahoda CA, et al. Effects of physiological electric fields on migration of human dermal fibroblasts. J Invest Dermatol. 2010;130:2320-7.

[76] Erickson CA, Nuccitelli R. Embryonic Fibroblast Motility and Orientation Can Be Influenced by Physiological Electric-Fields. J Cell Biol. 1984;98:296-307.

[77] Bourguignon G, Bourguignon L. Electric stimulation of protein and DNA synthesis in human fibroblasts. The FASEB Journal. 1987;1:398-402.

[78] Rouabhia M, Park H, Meng S, Derbali H, Zhang Z. Electrical stimulation promotes wound healing by enhancing dermal fibroblast activity and promoting myofibroblast transdifferentiation. PLoS One. 2013;8:e71660.

[79] Kloth LC. Electrical stimulation for wound healing: a review of evidence from in vitro studies, animal experiments, and clinical trials. The international journal of lower extremity wounds. 2005;4:23-44.

[80] Balakatounis KC, Angoules AG. Low-intensity electrical stimulation in wound healing: review of the efficacy of externally applied currents resembling the current of injury. Eplasty. 2008;8:e28.

[81] Alvarez OM, Mertz PM, Smerbeck RV, Eaglstein WH. The healing of superficial skin wounds is stimulated by external electrical current. J Invest Dermatol. 1983;81:144-8.

[82] MacDiarmid AG. “Synthetic metals”: A novel role for organic polymers (Nobel lecture). Angew Chem Int Ed. 2001;40:2581-90.

[83] Skobe M, Hamberg LM, Hawighorst T, Schirner M, Wolf GL, Alitalo K, et al. Concurrent induction of lymphangiogenesis, angiogenesis, and macrophage recruitment by vascular endothelial growth factor-C in melanoma. The American journal of pathology. 2001;159:893-903.

[84] Zhao M. Electrical fields in wound healing—an overriding signal that

directs cell migration. Semin Cell Dev Biol: Elsevier; 2009. p. 674-82.

[85] Sebastian A, Syed F, Perry D, Balamurugan V, Colthurst J, Chaudhry IH, et al. Acceleration of cutaneous healing by electrical stimulation: Degenerate electrical waveform down-regulates inflammation, up-regulates angiogenesis and advances remodeling in temporal punch biopsies in a human volunteer study. Wound Repair Regen. 2011;19:693-708.

[86] Roberts AB, Sporn MB, Assoian RK, Smith JM, Roche NS, Wakefield LM, et al. Transforming growth factor type beta: rapid induction of fibrosis and angiogenesis in vivo and stimulation of collagen formation in vitro. Proceedings of the National Academy of Sciences. 1986;83:4167-71.

[87] Silva R, D'Amico G, Hodivala-Dilke KM, Reynolds LE. Integrins The keys to unlocking angiogenesis. Atertio Thromb Vasc Biol. 2008;28:1703-13.

[88] Inkinen K, Turakainen H, Wolff H, Ravanti L, Kähäri VM, Ahonen J. Expression and activity of matrix metalloproteinase-2 and-9 in experimental granulation tissue. APMIS. 2000;108:318-28.

[89] AGAIBY AD, DYSON M. Immuno-inflammatory cell dynamics during cutaneous wound healing. J Anat. 1999;195:531-42.

[90] Sado Y, Kagawa M, Naito I, Ueki Y, Seki T, Momota R, et al. Organization and expression of basement membrane collagen IV genes and their roles in human disorders. J Biochem. 1998;123:767-76.

[91] Ud-Din S, Sebastian A, Giddings P, Colthurst J, Whiteside S, Morris J, et

al. Angiogenesis is induced and wound size is reduced by electrical stimulation in an acute wound healing model in human skin. PLoS One. 2015;10:e0124502.

[92] Cinar K, Comlekci S, Senol N. Effects of a specially pulsed electric field on an animal model of wound healing. Lasers Med Sci. 2009;24:735-40.

[93] Ristimäki A, Narko K, Enholm B, Joukov V, Alitalo K. Proinflammatory cytokines regulate expression of the lymphatic endothelial mitogen vascular endothelial growth factor-C. J Biol Chem. 1998;273:8413-8.

[94] Zykova SN, Jenssen TG, Berdal M, Olsen R, Myklebust R, Seljelid R. Altered cytokine and nitric oxide secretion in vitro by macrophages from diabetic type II-like db/db mice. Diabetes. 2000;49:1451-8.

[95] Leibovich S, Ross R. The role of the macrophage in wound repair. A study with hydrocortisone and antimacrophage serum. The American journal of pathology. 1975;78:71.

요약 (국문초록)

혈관은 몸 전체에 산소와 영양분을 공급하는 잘 정비된 체계이다. 혈관 체계에 장애가 생기면 말초동맥질환, 허혈성 심장질환, 허혈성 뇌졸중 등의 허혈성 질환이 발생한다. 이러한 허혈성 질환을 치료하기 위해서는, 효과적으로 혈관신생을 유도하여 허혈부위에 혈류를 공급하고 허혈성 손상으로부터 조직을 보호하는 것이 중요하다. 혈관신생은 창상 치료과정에서도 중요한 부분이다. 혈관신생은 창상 부위에 혈관 체계를 복구하고 치유과정에 참여하는 세포들에게 산소와 영양분을 공급하는 역할을 한다. 창상 치료과정에서 혈관신생에 문제가 생기면 재생이 지연되거나 상처가 만성창상으로 발전할 수 있다. 본 연구에서는 혈관신생을 유도하여 쥐의 하지허혈과 창상을 치료하기 위한 새로운 방법을 도입하였다.

3 장에서는, 인간 섬유육종 세포주인 HT1080 세포에서 얻은 조정배지를 쥐의 하지허혈 치료에 이용하였다. HT1080 세포의 조정배지의 성분과 효과는 인간 골수줄기세포 조정배지와 비교 분석 되었다. HT1080 세포 조정배지는 골수줄기세포 조정배지에 비해 높은 농도의 혈관신생 인자를 함유하고 있었다. 이는 골수줄기세포에 비해 훨씬 빠른 HT1080 세포의 증식속도 때문에

HT1080 세포의 농도가 더 높았기 때문이다. 이후 혈관신생 분석에서 HT1080 조정배지와 골수줄기세포 조정배지가 동일 세포 수에 근거 할 수 있도록 HT1080 조정배지를 희석하였다. 두 종류의 조정배지는, 배양접시에서 인간배꼽정맥내피세포의 생장을 촉진하였고 그 정도는 동일하였다. 허혈이 발생한 쥐의 하지에 HT1080 세포 조정배지를 주사 하였을 때, 모세혈관 밀도와 혈류가 신선한 배지를 주사했을 때와 비교하여 통계학적으로 유의미한 수준으로 향상되었다. HT1080 세포 조정배지는 골수줄기세포 조정배지와 비교하면 치료효과는 비슷하였지만, 종양세포의 빠른 증식과 제한 없는 생존 시간으로 인하여 조정배지를 준비하는데 있어 골수줄기세포에 비해 훨씬 효과적일 수 있다. 이러한 결과는 종양 세포를 혈관 신생과 허혈 질환 치료에 적용 할 수 있는 응용 가능성을 제시한다.

4 장에서는 피부 창상 치료를 촉진하기 위하여 피부에 부착 가능한 형태의 유기 태양전지 패치를 도입하였다. 전기장에 의한 전기자극은 피부 세포 및 면역 세포의 거동을 조절 할 수 있다. 본 연구자들이 제작한 패치는 쥐 등 부분의 상처에 부착되어, 흡수한 빛을 통해 지속적인 전기장을 전달한다. 동물 실험을 통해서 부착한

패치로 인해 상처부위의 혈관신생이 촉진되고, 세포의 생장과 사이토카인 분비, 단백질 합성이 강화되어 상처치료가 촉진됨을 확인하였다. 이 결과는 좀더 임상 적용이 용이하고, 환자 친화적인 창상 치료용 피부 부착 패치에 대한 접근을 가능하게 한다.

본 연구는 종양세포 조정배지와 유기태양전지 패치를 질환 치료에 이용하는 것이, 혈관 신생을 유도하고 치료효과를 기대 할 수 있는 효과적인 방법임을 증명하였다. 나아가 위 방법들은, 세포를 주사하지 않는 치료법이므로 임상적으로 적용이 용이하다.

주요어 : 혈관신생, 허혈성 질환, 조정배지, 피부창상, 유기태양전지
학번 : 2010-23356